



HAL
open science

Killing from the inside: Intracellular role of T3SS in the fate of *Pseudomonas aeruginosa* within macrophages revealed by *mgtC* and *oprF* mutants

Preeti Garai, Laurence Berry, Malika Moussouni, Sophie Bleves,
Anne-Béatrice Blanc-Potard

► To cite this version:

Preeti Garai, Laurence Berry, Malika Moussouni, Sophie Bleves, Anne-Béatrice Blanc-Potard. Killing from the inside: Intracellular role of T3SS in the fate of *Pseudomonas aeruginosa* within macrophages revealed by *mgtC* and *oprF* mutants. *PLoS Pathogens*, 2019, 10.1101/389718 . hal-02145586v1

HAL Id: hal-02145586

<https://amu.hal.science/hal-02145586v1>

Submitted on 5 Jul 2019 (v1), last revised 12 Sep 2019 (v2)

HAL is a multi-disciplinary open access archive for the deposit and dissemination of scientific research documents, whether they are published or not. The documents may come from teaching and research institutions in France or abroad, or from public or private research centers.

L'archive ouverte pluridisciplinaire **HAL**, est destinée au dépôt et à la diffusion de documents scientifiques de niveau recherche, publiés ou non, émanant des établissements d'enseignement et de recherche français ou étrangers, des laboratoires publics ou privés.



Distributed under a Creative Commons Attribution 4.0 International License

1 **Killing from the inside: Intracellular role of T3SS in the fate of *Pseudomonas***
2 ***aeruginosa* within macrophages revealed by *mgtC* and *oprF* mutants**

3

4 Preeti Garai ¹, Laurence Berry ^{1#}, Malika Moussouni^{1#}, Sophie Bleves², Anne-Béatrice Blanc-
5 Potard^{1*}

6

7 ¹Laboratoire de Dynamique des Interactions Membranaires Normales et Pathologiques,
8 Université de Montpellier, CNRS-UMR5235, Montpellier, France

9 ²LISM, Institut de Microbiologie de la Méditerranée, CNRS & Aix-Marseille Univ, Marseille,
10 France.

11

12 [#]Both authors contributed equally to the work

13

14 *Corresponding author:

15 **E-mail: anne.blanc-potard@umontpellier.fr**

16

17 Running title: Intramacrophage fate of *Pseudomonas aeruginosa*

18 **Abstract**

19

20 While considered solely an extracellular pathogen, increasing evidence indicates that
21 *Pseudomonas aeruginosa* encounters intracellular environment in diverse mammalian cell
22 types, including macrophages. In the present study, we have deciphered the intramacrophage
23 fate of wild-type *P. aeruginosa* PAO1 strain by live and electron microscopy. *P. aeruginosa*
24 first resided in phagosomal vacuoles and subsequently could be detected in the cytoplasm,
25 indicating phagosomal escape of the pathogen, a finding also supported by vacuolar rupture
26 assay. The intracellular bacteria could eventually induce cell lysis, both in a macrophage cell
27 line and primary human macrophages. Two bacterial factors, MgtC and OprF, recently
28 identified to be important for survival of *P. aeruginosa* in macrophages, were found to be
29 involved in bacterial escape from the phagosome as well as in cell lysis caused by
30 intracellular bacteria. Strikingly, type III secretion system (T3SS) genes of *P. aeruginosa*
31 were down-regulated within macrophages in both *mgtC* and *oprF* mutants. Concordantly,
32 cyclic di-GMP (c-di-GMP) level was increased in both mutants, providing a clue for negative
33 regulation of T3SS inside macrophages. Consistent with the phenotypes and gene expression
34 pattern of *mgtC* and *oprF* mutants, a T3SS mutant ($\Delta pscN$) exhibited defect in phagosomal
35 escape and macrophage lysis driven by internalized bacteria. Importantly, these effects
36 appeared to be largely dependent on the ExoS effector, in contrast with the known T3SS-
37 dependent, but ExoS independent, cytotoxicity caused by extracellular *P. aeruginosa* towards
38 macrophages. Moreover, this macrophage damage caused by intracellular *P. aeruginosa* was
39 found to be dependent on GTPase Activating Protein (GAP) domain of ExoS. Hence, our
40 work highlights T3SS and ExoS, whose expression is modulated by MgtC and OprF, as key
41 players in the intramacrophage life of *P. aeruginosa* which allow internalized bacteria to lyse
42 macrophages.

43

44 **Author summary**

45

46 The ability of professional phagocytes to ingest and kill microorganisms is central to
47 host defense and *Pseudomonas aeruginosa* has developed mechanisms to avoid being killed
48 by phagocytes. While considered an extracellular pathogen, *P. aeruginosa* has been reported
49 to be engulfed by macrophages in animal models. Here, we visualized the fate of *P.*
50 *aeruginosa* within cultured macrophages revealing macrophage lysis driven by intracellular
51 *P. aeruginosa*. Two bacterial factors, MgtC and OprF, recently discovered to be involved in
52 the intramacrophage survival of *P. aeruginosa*, appeared to play a role in this cytotoxicity
53 caused by intracellular bacteria. We provided evidence that type III secretion system (T3SS)
54 gene expression is lowered intracellularly in *mgtC* and *oprF* mutants. We further showed that
55 intramacrophage *P. aeruginosa* uses its T3SS, specifically the ExoS effector, to promote
56 phagosomal escape and cell lysis. We thus describe a transient intramacrophage stage of *P.*
57 *aeruginosa* that could contribute to bacterial dissemination.

58

59

60

61 **Introduction**

62

63 Pathogenic bacteria are commonly classified as intracellular or extracellular pathogens
64 [1]. Intracellular bacterial pathogens, such as *Mycobacterium tuberculosis* or *Salmonella*
65 *enterica*, can replicate within host cells, including macrophages. In contrast, extracellular
66 pathogens, such as *Yersinia* spp., *Staphylococcus aureus*, *Pseudomonas aeruginosa* or
67 streptococci, avoid phagocytosis or exhibit cytotoxicity towards phagocytic cells, to promote
68 their extracellular multiplication. However, recent data have emphasized that several
69 extracellular pathogens can enter host cells *in vivo*, resulting in a phase of intracellular
70 residence, which can be of importance in addition to the typical extracellular infection. For
71 example, although *Yersinia* spp. subvert the functions of phagocytes from the outside, these
72 bacteria also subvert macrophage functions within the cell [2]. Once considered an
73 extracellular pathogen, it is now established that *S. aureus* can survive within many
74 mammalian cell types including macrophages [3,4] and the intramacrophage fate of *S. aureus*
75 has been deciphered [5,6]. Moreover, an intracellular phase within splenic macrophages has
76 been recently shown to play a crucial role in initiating dissemination of *Streptococcus*
77 *pneumoniae*, providing a divergence from the dogma which considered this bacterial
78 pathogen the classical example of extracellular pathogens [7].

79

80 The environmental bacterium and opportunistic human pathogen *P. aeruginosa* is
81 responsible for a variety of acute infections and is a major cause of mortality in chronically
82 infected cystic fibrosis (CF) patients. The chronic infection of *P. aeruginosa* and its resistance
83 to treatment is largely due to its ability to form biofilms, which relies on the production of
84 exopolysaccharides (EPS), whereas the type III secretion system (T3SS) is reported to play a

85 key role in the pathogenesis of acute *P. aeruginosa* infections [8]. Four T3SS effectors
86 (ExoU, ExoS, ExoT, ExoY) have been identified so far, ExoS being nearly always mutually
87 exclusive with the potent cytotoxin ExoU and more prevalent than ExoU [9-11]. ExoS has a
88 dual function as it contains a GTPase activating (GAP) domain as well as an ADP
89 ribosyltransferase (ADPRT) domain [10]. An intracellular step in airway epithelial cells has
90 been proposed to occur before the formation of biofilm during the acute phase of infection
91 [12,13] and the intracellular stage of *P. aeruginosa* within cultured epithelial cells has been
92 fairly studied [14-16]. The principle that *P. aeruginosa* is not exclusively an extracellular
93 pathogen has been convincingly established by the recent use of advanced imaging methods
94 to track bacteria within epithelial cells [17]. The T3SS, more specifically its effector ExoS,
95 has been implicated in the formation of membrane blebs-niche and avoidance of acidified
96 compartments to allow bacterial multiplication within epithelial cells [17-19]. Concordantly,
97 T3SS genes were recently shown to be expressed in *P. aeruginosa* internalized in epithelial
98 cells [17]. Regarding the interaction with macrophages, *P. aeruginosa* has developed
99 mechanisms to avoid phagocytosis [20]. However, *P. aeruginosa* has been shown to be
100 phagocytosed by macrophages in an acute model of infection in zebrafish embryos [21,22]
101 and has been reported to be engulfed by alveolar macrophages in the lungs of mice early after
102 pulmonary infection [23], suggesting that *P. aeruginosa* may need strategies to escape
103 macrophage killing. Although *P. aeruginosa* has been localized within cultured macrophages
104 during gentamicin protection assays [24-26], the intramacrophage fate of the bacteria has not
105 been characterized and bacterial factors involved in this step remain largely unexplored.

106

107 Bacterial survival in a particular niche requires the development of an adaptive
108 response, generally mediated by regulation of the bacterial genes involved in physiological
109 adaptation to the microenvironment. The identification of mutants lacking the ability to

110 survive within macrophages and the study of *P. aeruginosa* gene expression inside
111 macrophages is critical to determine bacterial players in this step. We have previously
112 uncovered MgtC as a bacterial factor involved in the intramacrophage survival of *P.*
113 *aeruginosa* [25,27]. In agreement with this intramacrophage role, expression of *Pseudomonas*
114 *mgtC* (PA4635) gene is induced when the bacteria reside inside macrophages [25]. MgtC is
115 known to promote intramacrophage growth in several classical intracellular bacteria,
116 including *Salmonella typhimurium* where it inhibits bacterial ATP synthase and represses
117 cellulose production [28-30], and is considered as a clue to reveal bacterial pathogens adapted
118 to an intramacrophage stage [30,31]. In addition, a recent study has implicated the outer
119 membrane protein OprF in the ability of otopathogenic *P. aeruginosa* strains to survive inside
120 macrophages [26]. OprF is an outer membrane porin that can modulate the production of
121 various virulence factors of *P. aeruginosa* [32,33].

122

123 In the present study, we investigated the fate of *P. aeruginosa* within macrophages
124 using wild-type PAO1 strain, which lacks ExoU, along with isogenic *mgtC* and *oprF* mutants.
125 We also explored, for the first time, the regulation of T3SS genes when *P. aeruginosa* resides
126 inside macrophages. The T3SS and ExoS effector, whose expression was found to be
127 modulated by MgtC and OprF intracellularly, were seemingly involved in this intracellular
128 stage, playing a role in vacuolar escape and cell lysis caused by intracellular bacteria.

129

130 **Results**

131

132 **Intracellular *P. aeruginosa* can promote macrophage lysis**

133 We previously visualized fluorescent *P. aeruginosa* residing within fixed macrophages [25].
134 To investigate the fate of *P. aeruginosa* after phagocytosis in a dynamic way, we monitored
135 macrophages infected with fluorescent bacteria using time-lapse live microscopy. J774
136 macrophages were infected with wild-type PAO1 strain expressing GFP grown exponentially
137 in LB medium (Multiplicity of infection or MOI=10). After 25 minutes of phagocytosis,
138 several washes were performed to remove adherent bacteria and gentamicin was added to kill
139 extracellular bacteria. Microscopic observation of infected macrophages up to 3 hours showed
140 cell lysis with increasing time (Fig 1), starting between 1.5 and 2 hours post-phagocytosis,
141 which can be attributed to intracellular bacteria as gentamicin was retained throughout the
142 experiment. No lysis of uninfected cells present in the same field was observed (Fig 1 and S1
143 Fig), as expected from an event due to intracellular bacteria rather than extracellular bacteria.
144 The cell lysis appeared to take place within a rapid time frame of few seconds, as shown by
145 the movie (S1 Movie), after which the bacteria seemed to be released from the host cell. We
146 also infected human monocyte-derived macrophages (HMDMs) with GFP producing PAO1
147 strain under similar conditions and found lysed infected cells after 2 hours of phagocytosis
148 (S2 Fig). Hence, the phenomenon of lysis of macrophages by intracellular PAO1 is not
149 restricted to J774 cell line, but is extendable to primary human macrophages.

150

151 We further examined intracellular *P. aeruginosa* within macrophages in more detail
152 using transmission electron microscopy (TEM). J774 macrophages infected with wild-type
153 PAO1 strain, were subjected to fixation at early time post-infection (30 min after
154 phagocytosis) or at later time of infection (3 hrs after phagocytosis). After phagocytosis, *P.*
155 *aeruginosa* was present in membrane bound vacuoles inside macrophages (Fig 2A). At a later
156 time point, some bacteria could be found in the cytoplasm with no surrounding membrane,
157 suggesting disruption of the vacuole membrane (Fig 2B). The infected macrophage was

158 damaged, displaying highly condensed chromatin and membrane blebbing, and lacking
159 pseudopodia. Healthy infected cells were also observed, where bacteria were mostly found in
160 vacuoles partially or totally filled with heterogeneous electron dense material, suggesting that
161 the vacuole has fused with lysosomes (Fig 2C). To confirm this, we examined the association
162 between fluorescent PAO1 bacteria and the LysoTracker probe during infection using fixed
163 macrophages. Bacteria colocalizing with LysoTracker could be visualized (S3 Fig), thereby
164 corroborating the TEM observation of fusion of vacuoles with lysosomes and the localization
165 of bacteria in acidified compartment.

166 TEM analyses allowed us to conclude that wild-type PAO1 strain has the ability to
167 reside within vacuoles and possibly escape from the phagosome into the cytoplasm and
168 promote cell damage. A rapid cell lysis event caused by intracellular *P. aeruginosa* visualized
169 by live microscopy revealed that phagocytosed bacteria can escape from macrophage through
170 cell lysis.

171

172 **Intracellular *mgtC* and *oprF* mutants are compromised in cell lysis**

173 Our previous results based on gentamicin protection assay on J774 infected macrophages and
174 counting of colony forming units (CFU) indicated that *mgtC* mutant (generated in the PAO1)
175 background) survived to a lesser extent than the wild-type strain [25]. More recently, an *oprF*
176 mutant of an otopathogenic strain of *P. aeruginosa* was also found to be defective in
177 intracellular survival in mouse bone marrow macrophages based on gentamicin protection
178 assay [26]. To analyze the phenotypes of *oprF* mutant in the PAO1 background towards J774
179 macrophages and compare that with *mgtC* mutant, we used here a previously described *oprF*
180 mutant generated in PAO1 strain [25,34].

181 Based on the finding that intracellular *P. aeruginosa* can cause macrophage lysis, we
182 developed a suitable assay using fluorescent microscopic analysis to quantify cell damage
183 caused by intracellular bacteria. Macrophages were infected with fluorescent bacteria, treated
184 with gentamicin for 2 hours after phagocytosis, fixed and stained with phalloidin-TRITC to
185 label F-actin and visualize macrophage morphology. A clear cortical red labeling was seen in
186 most cells, which is indicative of the plasma membrane-associated cortical actin. Few infected
187 cells appeared lysed due to the loss of cortical actin staining (Fig 3A), which agrees with the
188 observation of lysed macrophages in time lapse fluorescence microscopy (Fig 1). The loss of
189 cortical actin staining was found to be due to internalized bacteria because upon arresting
190 phagocytosis, by treating macrophages with cytochalasin D, bacteria were not internalized
191 and loss of cortical actin staining was not observed (S4 Fig). Hence, any delayed effect of
192 extracellular bacteria occurring before gentamicin treatment or a contribution of extracellular
193 bacteria that would resist gentamicin treatment can be ruled out. Quantification of the number
194 of cells without phalloidin labelling showed highest value for wild-type strain, intermediate
195 for *mgtC* mutant and lowest for *oprF* mutant (Fig 3B). Thus, both intracellular *mgtC* and *oprF*
196 mutants appeared compromised for cell lysis. This feature is not linked to a lower
197 internalization rate of the mutant strains, because *mgtC* mutant is known to be more
198 phagocytosed than wild-type strain [25] and a similar trend was found for *oprF* mutant (not
199 shown). Since T3SS has been involved in the intracellular life of *P. aeruginosa* in other cell
200 types [17], we next monitored the expression of T3SS genes during the residence of bacteria
201 within macrophages.

202

203 **Down-regulation of T3SS gene expression in *mgtC* and *oprF* mutants inside**
204 **macrophages**

205 The *P. aeruginosa oprF* mutant was reported to be defective in the secretion of T3SS
206 effectors in liquid culture and in the production of PcrV, the T3SS needle tip protein [32,34],
207 but the effect of OprF on transcription of T3SS genes has not been tested so far. We thus
208 investigated the expression of the effector gene *exoS* along with the gene *pcrV* in *oprF* mutant
209 strain in comparison to wild-type strain upon macrophage infection. As a control, we tested
210 flagellin coding gene *fliC*, which is not part of the T3SS regulon, but was proposed to be
211 secreted by the T3SS [35]. Expression of both *pcrV* and *exoS* genes was found to be highly
212 reduced in the *oprF* mutant (Fig 4). Strikingly, the *mgtC* mutant also exhibited significantly
213 reduced expression of these two T3SS genes (Fig 4), although to a lesser extent than the *oprF*
214 mutant, indicating an unexpected interplay between MgtC and T3SS. On the other hand, *fliC*
215 expression was not altered in both mutants.

216 Since we observed a decreased transcriptional level of T3SS genes in the *oprF* mutant,
217 we further examined the link between intramacrophage expression of T3SS and cell lysis in
218 this mutant. A recombinant plasmid allowing IPTG-inducible overproduction of ExsA, a
219 master transcriptional activator of T3SS genes [36], was introduced in the *oprF* mutant. Upon
220 induction of *exsA* expression with 0.01 mM IPTG, *oprF* mutant promoted macrophage lysis
221 like the wild-type strain (S5 Fig), supporting a model whereby the effect of OprF is the result
222 of its positive regulatory effect on T3SS expression.

223 To address the mechanism behind the downregulation of transcription of T3SS in *oprF*
224 and *mgtC* mutant strains, we evaluated the level of the second messenger c-di-GMP, as it is
225 known to participate in T3SS repression in *P. aeruginosa* [37]. The *oprF* mutant was already
226 reported to have high production of c-di-GMP in liquid culture [34]. We used a fluorescence-
227 based reporter (Fig 5A) that has been validated to gauge c-di-GMP level inside *P. aeruginosa*
228 [38]. The pCdrA::*gfp* plasmid was introduced into wild-type and mutant strains, and
229 fluorescence was measured in infected macrophages (Fig 5B). Both *oprF* and *mgtC* mutants

230 exhibited significantly increased activity of the *cdrA* promoter comparatively to wild-type
231 strain, indicative of higher levels of c-di-GMP than the wild-type strain. To better appreciate
232 the differences monitored within macrophages, we also measured fluorescence of strains
233 grown in culture medium with various magnesium concentrations (Fig 5C). The *oprF* mutant
234 exhibited a two to three-fold increase in the activity of the *cdrA* promoter comparatively to
235 wild-type strain, which is in the same range as the increase observed within macrophages (Fig
236 5B), and agrees with published data obtained with this indirect strategy and direct c-di-GMP
237 measurement [34]. Under magnesium limitation, a condition known to induce the expression
238 of *mgtC*, the *mgtC* mutant also showed increased activity of the *cdrA* promoter comparatively
239 to wild-type strain, with a two-fold increase in the absence of Mg^{2+} , and a minor, but
240 significant, increase in the presence of 10 μM Mg^{2+} that is similar to what is observed within
241 macrophages. On the other hand, the level of fluorescence of wild-type strain and *mgtC*
242 mutant was identical in medium supplemented with 1 mM Mg^{2+} , a condition that prevents
243 *mgtC* expression [25]. Taken together, these results indicate that the production of c-di-GMP
244 is increased relatively to wild-type strain in both *oprF* and *mgtC* mutants, with a more
245 pronounced effect for *oprF*, when bacteria reside within macrophages, thus providing a
246 mechanistic clue for the negative effect on T3SS gene expression.

247

248 **A T3SS mutant is defective for cell death driven intracellularly in an ExoS-dependent** 249 **manner**

250 Given the effect of both *oprF* and *mgtC* deletions on the expression of T3SS genes within
251 macrophages, we investigated the fate of a T3SS mutant upon phagocytosis. We first used a
252 *pscN* mutant that is defective for the ATPase function of the T3SS machinery [36].
253 Intracellular T3SS mutant did not induce loss of cortical phalloidin staining, as shown by
254 fluorescent imaging and subsequent quantification, indicating lack of cell lysis (Fig 6A and

255 B). Thus, the phenotype of T3SS mutant is consistent with that of *mgtC* and *oprF* mutants and
256 in correlation with their level of T3SS gene expression. We further examined the relevance of
257 our findings to primary human macrophages, by assessing the lysis of HMDMs driven
258 intracellularly by wild-type *P. aeruginosa* or *oprF* and *pscN* mutants. The count of
259 intracellularly lysed cells was significantly different between wild-type and each mutant strain
260 (Fig 7), with a similar trend to that of J774 macrophages (Fig 3 and Fig 6), thus confirming
261 the importance of T3SS in intracellularly driven lysis of primary macrophages as well.

262

263 To address the implication of T3SS effector proteins in this process, we used
264 individual effector mutant strains *exoS*, *exoT*, *exoY* and the triple mutant *exoSTY*. The
265 intracellular lysis of macrophages was found to be reduced for the triple mutant *exoSTY* and
266 to a similar extent for the *exoS* mutant (Fig 6A and B), suggesting a major contribution of
267 ExoS. Accordingly, *exoT* and *exoY* mutants behave similarly to wild-type strain (Fig 6B).
268 Moreover, complementation of the *exoSTY* mutant with *exoS* restored the wild-type
269 phenotype (Fig. 6C). Although the lysis by *exoS* mutant strain was substantially higher than
270 that of *pscN* mutant, these results suggest that the T3SS-mediated intracellular lysis of
271 macrophages by *P. aeruginosa* relies mainly on the T3SS effector ExoS. Thus, this ExoS-
272 dependent cytotoxic effect mediated by intracellular bacteria differs from the classical T3SS-
273 dependent cytotoxicity driven by extracellular bacteria towards macrophages that has been
274 reported to be mostly independent of ExoS [39-41]. To confirm this difference between
275 intracellular and extracellular bacteria mediated lysis, we measured the lactate dehydrogenase
276 (LDH) release when infection was carried out without removing extracellular bacteria. As
277 expected, similar values were obtained for wild-type strain and *exoS* mutant, whereas a *pscN*
278 mutant showed significantly reduced LDH release (S6 Fig), which agrees with the reported
279 T3SS-dependent but ExoS independent cytotoxicity caused by extracellular bacteria. This is

280 consistent with trypan blue exclusion assay, which monitors cell death based on penetration of
281 a membrane impermeable dye, when the assay is done immediately after phagocytosis (S7
282 Fig, panel A).

283 ExoS possesses both GAP domain as well as ADPRT domain and complementing
284 strains retaining only one of these two domains have been constructed earlier [42]. To address
285 which domain of ExoS plays role in intracellular cytotoxicity, we carried out the phalloidin-
286 based lysis assay using the *exoSTY* mutant producing either ADPRT (GAP-) or GAP
287 (ADPRT-) domain of ExoS. Our results clearly showed that the strain retaining GAP activity
288 of ExoS but lacking ADPRT activity (Δ *exoSTY* + *exoS* ADPRT-) could complement the
289 phenotype to an extent similar to the strain complemented with *exoS* (Fig. 6C), which is also
290 equivalent to the wild-type. To strengthen our findings, we performed trypan blue exclusion
291 assay after 2hrs of gentamicin treatment. The results are consistent with phalloidin assay,
292 supporting the implication of ExoS, and more specifically its GAP domain, for macrophage
293 death induced by intracellular bacteria (S7 Fig, panel B). This contrasts with the results of
294 trypan blue exclusion assay performed immediately after phagocytosis, where a low level of
295 T3SS-dependent cell death is observed, but not linked to ExoS function (S7 Fig, panel A).

296 Hence, our results indicate that, in contrast to extracellular *P. aeruginosa*, intracellular
297 *P. aeruginosa* uses an ExoS-dependent T3SS mediated mechanism to promote macrophage
298 lysis. Moreover, only the GAP activity of ExoS is required for this process.

299

300 ***P. aeruginosa* T3SS, *oprF* and *mgtC* mutants displayed lower vacuolar escape than wild- 301 type PAO1**

302 The phagosomal environment of the macrophage is hostile for bacterial pathogens and TEM
303 analysis indicated that PAO1 can be found in the cytoplasm, suggesting escape from the

304 phagosomal vacuole (Fig 2B). We decided to address the intracellular role of T3SS, OprF and
305 MgtC in the phagosomal escape of *P. aeruginosa* to the cytoplasm of macrophages. To
306 monitor *P. aeruginosa* escape from phagosome, we used the CCF4-AM/ β -lactamase assay
307 that has been developed for tracking vacuolar rupture by intracellular pathogens [43]. This
308 assay takes advantage of the natural production of β -lactamase by *P. aeruginosa* [44], which
309 can cleave a fluorescent β -lactamase substrate, CCF4-AM, that is trapped within the host
310 cytoplasm. CCF4-AM emits a green fluorescence signal, whereas in the presence of β -
311 lactamase activity, a blue fluorescence signal is produced. The detection of blue fluorescent
312 cells at 2 hrs post-phagocytosis indicated bacterial escape from the phagosome to the
313 cytoplasm (Fig 8A). The escape of wild-type strain was compared to that of *mgtC*, *oprF* and
314 *pscN* mutants by quantifying the percentage of blue fluorescent cells out of total green
315 fluorescent cells. Wild-type strain showed significantly higher percentage of phagosomal
316 escape than all mutants tested (Fig 8B). No significant difference in terms of cleavage of
317 CCF4-AM was measured for the mutants with respect to wild-type in liquid cultures (S8 Fig),
318 indicating that the lower amount of blue fluorescent cells with the mutants is not due to
319 reduced production of endogenous β -lactamase. In agreement with the finding of phagosomal
320 escape by CCF4-AM/ β -lactamase assay, ruptured phagosomal membrane could be visualized
321 by TEM in macrophages infected with PAO1 wild-type strain (Fig 8C). Both *exoS* and
322 *exoSTY* effector mutants also displayed a low percentage of phagosomal escape, which
323 appeared similar to that of *pscN* mutant (S9 Fig). These results indicate that the T3SS,
324 through the ExoS effector, plays role in the escape of *P. aeruginosa* from the phagosome to
325 the cytoplasm. The effect of MgtC and OprF in this process may as well be mediated by their
326 effect on T3SS gene expression (Fig 4).

327 Cumulatively, our results support a T3SS-dependent vacuolar escape for *P.*
328 *aeruginosa*, leading to the localization of bacteria in the cytoplasm and cell lysis as depicted
329 in the proposed model (Fig 9).

330

331 **Discussion**

332

333 The ability of professional phagocytes to ingest and kill microorganisms is central to
334 innate immunity and host defense. *P. aeruginosa* is known to avoid being killed by
335 phagocytes through the destruction of immune cells extracellularly as well as avoidance of
336 phagocytosis [20]. However, *P. aeruginosa* has been reported to be engulfed by macrophages
337 in animal infection models [21-23]. In addition, *P. aeruginosa* has been visualized in
338 phagocytes in cell culture models in several studies, where MgtC and OprF have been shown
339 to be involved in the ability of *P. aeruginosa* to survive in cultured macrophages [25,26]. The
340 virulence of *P. aeruginosa mgtC* mutant can be restored in zebrafish embryos upon
341 macrophages depletion, suggesting that MgtC acts to evade phagocytes [25]. Interestingly, a
342 similar behavior has been reported for a T3SS mutant in the same infection model [21]. We
343 show here that MgtC and OprF regulate T3SS when *P. aeruginosa* resides in macrophages
344 and we describe a novel strategy used by *P. aeruginosa* to escape from macrophages that
345 relies on a T3SS-dependent cell lysis induced by intracellular bacteria (Fig. 9).

346

347 Using electron microscopy, we demonstrate that upon phagocytosis, *P. aeruginosa*
348 PAO1 strain resides in membrane bound vacuoles, whereas a cytosolic location can be
349 observed at later time of infection, which corroborates the observation of an otopathogenic *P.*
350 *aeruginosa* clinical strain in HMDMs [26]. Microscopic analysis of live and fixed cells

351 revealed macrophage lysis driven by intracellular bacteria, both with J774 macrophage cell
352 line as well as HMDMs. This cell lysis is a rapid process associated with the loss of cortical
353 actin from plasma membrane. We propose that the cell lysis induced by intracellular *P.*
354 *aeruginosa* is linked to the phagosomal escape of bacteria as indicated by the observation of
355 cytosolic bacteria and ruptured phagosomal membrane by TEM as well as CCF4-AM/ β -
356 lactamase based phagosomal rupture assay.

357

358 To better characterize the *P. aeruginosa* factors involved in its intramacrophage fate,
359 we investigated intracellular expression of T3SS genes in *mgtC* and *oprF* mutants. Expression
360 of T3SS genes upon macrophage infection was significantly decreased in *mgtC* mutant and
361 abrogated in *oprF* mutant. The production of T3SS effectors or needle component was
362 previously known to be altered in the *oprF* mutant [32,34], but a direct effect at the
363 transcriptional level was not investigated before. This regulation could be mediated by c-di-
364 GMP, a known negative regulator of T3SS expression [37], as the reporter assay revealed an
365 increased level of c-di-GMP in both *oprF* and *mgtC* mutants upon monitoring infected
366 macrophages, with a more pronounced effect for *oprF* mutant. An increased level of c-di-
367 GMP in *oprF* mutant is consistent with previous results obtained *in vitro* [34]. The moderate,
368 but significant, increased level of c-di-GMP in *mgtC* mutant in macrophages with respect to
369 wild-type strain is equivalent to the fold increase obtained in low-Mg²⁺ cultures. It is of
370 interest to note that a *Salmonella mgtC* mutant also exhibited increased c-di-GMP level
371 intracellularly and under low-Mg²⁺ condition [29]. The *P. aeruginosa mgtC* and *oprF* mutants
372 showed a moderate and a more pronounced decrease, respectively, in cytotoxicity driven by
373 intracellular bacteria and phagosomal escape. These phenotypes could be linked to the pattern
374 of T3SS expression in *mgtC* and *oprF* mutants, because a T3SS mutant appeared to lack
375 cytotoxicity driven by intracellular bacteria and showed reduced phagosomal escape.

376 Accordingly, inducing expression of *exsA* gene, a master activator of T3SS, in *oprF* mutant
377 promoted macrophage lysis driven by intracellular bacteria to a similar level to that of wild-
378 type strain, supporting the model whereby the phenotype of *oprF* mutant is the result of a
379 negative regulation of T3SS expression.

380

381 Our data indicate that the T3SS-mediated cytotoxicity driven by intracellular *P.*
382 *aeruginosa* is largely dependent on the ExoS effector. ExoS, which has a dual function [10],
383 is known to play a role in *P. aeruginosa* intracellular life in cell types other than
384 macrophages. The T3SS and ExoS are indeed key factors for intracellular replication of *P.*
385 *aeruginosa* in epithelial cells, with a main role of the ADPRT domain in the formation of
386 replicative niche in membrane blebs [18,19,45]. ExoS and ExoT ADPRT domains also
387 promote bacterial survival in neutrophils [46], by having a protective role against NADPH-
388 oxidase activity [47]. However, the effect of T3SS towards macrophages was so far restricted
389 to the well-known cytotoxicity caused by extracellular *P. aeruginosa* [39,48-50]. In *P.*
390 *aeruginosa* strains lacking ExoU toxin, such as PAO1, this cytotoxicity is due to
391 inflammasome activation, which is dependent on T3SS translocation apparatus, but is
392 independent of the ExoS effector [39-41,51]. Accordingly, this T3SS-dependent ExoS-
393 independent cytotoxicity was observed in our assays when extracellular bacteria are not
394 removed. In contrast, upon removal of extracellular bacteria, a T3SS-mediated cytotoxicity
395 implicating ExoS was uncovered. Hence, ExoS appears to be associated with cell damage
396 only when it is secreted from internalized bacteria. Moreover, phagosomal rupture assay
397 indicated that ExoS plays role in the escape of *P. aeruginosa* from the phagosome to the
398 cytoplasm and we propose that upon phagosomal rupture, the cytoplasmic location of *P.*
399 *aeruginosa* induces inflammasome, possibly through the release of bacterial
400 lipopolysaccharides (LPS) in the cytoplasm, which would promote cell death. Therefore, in

401 addition to the inflammasome activation caused by extracellular *P. aeruginosa* and, as very
402 recently described, by intracellular T3SS-negative *P. aeruginosa* in the context of long-term
403 infection [52], our study suggests that inflammasome and subsequent macrophage death can
404 also be caused by intracellular T3SS-positive *P. aeruginosa*. Further experiments will be
405 required to characterize inflammasome activation and pathways that lead to cell death.

406

407 The intracellular implication of ExoS in both macrophages and epithelial cells
408 suggests that the intracellular life of *P. aeruginosa* in macrophages shares features with the
409 intracellular life of the pathogen in epithelial cells, even though the outcome is different.
410 Whereas bacteria actively replicate in epithelial cells, within bleb niches or in the cytosol
411 [17], replication of bacteria is barely seen within macrophages resulting instead in cell lysis
412 and bacterial escape from macrophages. Our results further indicate that the macrophage
413 damage caused by intracellular bacteria is due to ExoS GAP domain, which thus differs from
414 the reported role of the ADPRT domain of ExoS in blebs formation associated with *P.*
415 *aeruginosa* intracellular replication within epithelial cells [18,19,45]. On the other hand, the
416 implication of GAP domain of ExoS towards epithelial cells in promoting cell rounding, actin
417 reorganization or cell death has not been specifically associated with intracellular bacteria
418 [53,54]. Although ExoS and ExoT GAP domain have similar biochemical activities, these
419 effectors may differ in their localization inside host cells or they may interact with different
420 host factors to bring about their effect. This is supported by the fact that induction of
421 apoptosis in epithelial cells by ExoT GAP domain, a feature that was not reported for ExoS
422 GAP domain [55] and by our finding that, unlike ExoS, ExoT is not involved in the
423 intramacrophage phenotypes. Importantly, we showed that the extent of phagosomal escape
424 of *pscN* and *exoSTY* mutants was similar to that of *exoS* mutant alone, suggesting that ExoS is
425 the main effector protein involved in the exit of *P. aeruginosa* from the phagosome. In

426 epithelial cells, ExoS has been involved in avoidance of acidified compartment [18,19].
427 Considering our findings, ExoS may allow avoidance of acidification in macrophages and
428 may also contribute to the vacuolar escape in epithelial cells. Further studies will be required
429 to decipher in more detail, the function of ExoS inside macrophages, including a better
430 understanding of its role in phagosomal escape and identification of its host targets within
431 macrophages. ExoS-positive strains represent a large amount of clinical isolates but the
432 number of ExoS-negative strains is nevertheless substantial (about one third of isolates),
433 especially among strains associated with bacteremia [10,11,56]. However, strains lacking
434 ExoS usually encode the potent cytotoxin ExoU, thus exhibiting high toxicity towards
435 eukaryotic cells from outside and less susceptibility to encounter an intracellular stage.

436

437 In conclusion, our results indicate that *P. aeruginosa* shares common feature with
438 other so-called extracellular pathogens, such as *S. aureus*, which can reside transiently within
439 macrophages [4] and require bacterial factors to survive this stage [57]. The present study
440 uncovered bacterial factors allowing internalized *P. aeruginosa* to lyse macrophages. This
441 should allow bacteria to evade macrophages and an important issue now is to better evaluate
442 the contribution of intramacrophage stage to disease outcome during *P. aeruginosa* infection.
443 Survival of *P. aeruginosa* within macrophages and subsequent bacterial release may play a
444 role in the establishment and dissemination of infection. There is also evidence that
445 intracellular survival may contribute to persistence of the infection by creating a niche
446 refractory to antibiotic action [24], highlighting the potential importance of this overlooked
447 phase of *P. aeruginosa* infection.

448

449 **Materials and methods**

450

451 **Bacterial strains and growth conditions**

452 Bacterial strains and plasmids are described in Table 1. *P. aeruginosa* mutant strains (all in
453 the PAO1 background) have been described and phenotypically characterized previously
454 (Table 1). The *oprF* mutant (strain H636) is derived from PAO1 wild-type strain H103 [34],
455 which exhibits the same level of ExoS secretion under T3SS-inducing conditions as PAO1,
456 isogenic strain for *mgtC* and T3SS mutants (S10 Fig). *P. aeruginosa* was grown at 37°C in
457 Luria broth (LB). Growth in magnesium-defined medium was done in NCE-minimal medium
458 [58] supplemented with 0.1% casamino acids, 38 mM glycerol, without MgSO₄ or containing
459 10 μM or 1mM MgSO₄. Plasmid pMF230 expressing GFP constitutively [59] (obtained from
460 Addgene), was introduced in *P. aeruginosa* by conjugation, using an *E. coli* strain containing
461 helper plasmid pRK2013. Recombinant bacteria were selected on *Pseudomonas* isolation agar
462 (PIA) containing carbenicillin at the concentration of 300 μg/ml.

463

464 **Table 1. Bacterial strains and plasmids used in the study**

Name	Description	Reference
PAO1		Laboratory collection
PAO1 $\Delta mgtC$	$\Delta mgtC$	[25]
H636	$\Delta oprF$	[34]
PAO1 $\Delta pscN$	$\Delta pscN$ T3SS ATPase mutant	[36]
PAO1 $\Delta exoS$	$\Delta exoS$	[50]

PAO1 Δ <i>exoY</i>	Δ <i>exoY</i>	[50]
PAO1 Δ <i>exoT</i>	Δ <i>exoT</i>	[50]
PAO1 Δ <i>exoSTY</i>	Δ <i>exoSTY</i>	[50]
PAO1F Δ 3Tox/ExoS	Δ <i>exoS</i> Δ <i>exoT</i> Δ <i>exoY</i> <i>attB::exoS</i>	[42]
PAO1F Δ 3Tox/ExoS _{GAP-}	Δ <i>exoS</i> Δ <i>exoT</i> Δ <i>exoY</i> <i>attB::exoS-R_{146K}</i>	[42]
PAO1F Δ 3Tox/ExoS _{ADPR-}	Δ <i>exoS</i> Δ <i>exoT</i> Δ <i>exoY</i> <i>attB::exoS-E_{379D}/E_{381D}</i>	[42]
pRK2013	Tra ⁺ , Mob ⁺ , ColE1, Km ^r	Laboratory collection
pMF230	GFP _{mut2} , Amp ^r	[59]
pTn7CdrA:: <i>gfp^C</i>	Amp ^r , Gm ^r	[38]
pSBC6	<i>exsA</i> cloned in pMMB190 under control of <i>tacp</i> Amp ^r	[36]

465

466

467 **Infection of J774 macrophages**

468 J774 cells (mouse macrophage cell line J774A.1, gifted by Gisèle Bourg, Inserm U 1047,
469 Nîmes, France) were maintained at 37°C in 5% CO₂ in Dulbecco's modified Eagle medium
470 (DMEM) (Gibco) supplemented with 10% fetal bovine serum (FBS) (Gibco). The infection of
471 J774 macrophages by *P. aeruginosa* was carried out essentially as described previously [25].

472 Mid-log phase *P. aeruginosa* grown in LB broth was centrifuged and resuspended in PBS to
473 infect J774 macrophages (5×10^5 cells/well) at an MOI of 10. After centrifugation of the 24-
474 well culture plate for 5 min for synchronization of infection, bacterial phagocytosis was
475 allowed for 25 min. Cells were washed three times with sterile PBS and fresh DMEM
476 medium supplemented with 400 $\mu\text{g/ml}$ gentamicin was added and retained throughout the
477 infection.

478

479 **Infection of Human Primary Macrophages**

480 Purified monocytes isolated as described from blood of healthy donors were frozen in liquid
481 nitrogen [60,61]. Cells were thawed for experiment and seeded onto 24-well plates at a
482 density of 7×10^5 per well in complete culture medium (RPMI containing 10% FCS) and
483 differentiated into macrophages with rh-M-CSF (10 ng/ml) (purchased from Al-Immuno
484 tools) for 7 days. HMDMs were infected with exponentially growing *P. aeruginosa* cultures
485 ($\text{DO}_{600}=0.8$) at a multiplicity of infection (MOI) of 10:1, as described above.

486

487 **Live microscopy**

488 J774 macrophages were seeded in ibidi μ slide (8 wells) in DMEM medium supplemented
489 with 10% FBS and infected with *P. aeruginosa* PAO1 expressing GFP as described in the
490 previous section. Imaging started after 30 min of phagocytosis, when the media was changed
491 to DMEM supplemented with 400 $\mu\text{g/ml}$ gentamicin until 3 hrs post phagocytosis. Cells were
492 imaged using an inverted epifluorescence microscope (Axioobserver, Zeiss), equipped with
493 an incubation chamber set-up at 37°C and 5% CO_2 and a CoolSNAP HQ2 CCD camera
494 (Photometrics). Time-lapse experiments were performed, by automatic acquisition of random

495 fields using a 63X Apochromat objective (NA 1.4). The frequency of acquisition is indicated
496 in figure legends. Image treatment and analysis were performed using Zen software (Zeiss).

497

498 **Transmission Electron microscopy**

499 Macrophages were seeded on glass coverslips and infected as described above. Infected cells
500 were fixed for 4 hrs at room temperature with 2.5% gluteraldehyde in cacodylate buffer 0.1 M
501 pH 7.4 with 5mM CaCl₂, washed with cacodylate buffer, post-fixed for 1 hr in 1% osmium
502 tetroxide and 1.5 % potassium ferricyanide in cacodylate buffer, washed with distilled water,
503 followed by overnight incubation in 2% uranyl acetate, prepared in water. Dehydration was
504 performed through acetonitrile series and samples were impregnated in epon 118: acetonitrile
505 50:50, followed by two times for 1 hr in 100% epon. After overnight polymerization at 60°C,
506 coverslips were detached by thermal shock with liquid nitrogen. Polymerization was then
507 prolonged for 48 hrs at 60°C. Ultrathin sections of 70 nm were cut with a Leica UC7
508 ultramicrotome (Leica microsystems), counterstained with lead citrate and observed in a Jeol
509 1200 EXII transmission electron microscope. All chemicals were from Electron Microscopy
510 Sciences (USA) and solvents were from Sigma. Images were processed using Fiji software.

511

512 **Colocalization of *P. aeruginosa* with acidic compartments**

513 Macrophages were infected with GFP labelled *P. aeruginosa* as described above. After 2.5
514 hrs of gentamicin treatment, infected J774 cells were washed twice with PBS and incubated
515 with 50 nM LysoTracker red DND-99 (Molecular Probes) in DMEM for 10 min to stain
516 lysosomes. Cells were then washed with PBS and fixed with 4% paraformaldehyde in PBS
517 and mounted on glass slides in Vectashield (Vector Laboratories, Inc) with 4',6-diamidino-2-
518 phenylindole (DAPI) to stain the nucleus. The slides were examined using an upright

519 fluorescence microscope (Axioimager Z2, Zeiss) equipped with an Apotome 1 for optical
520 sectioning. A 63X Apochromat Objective (NA 1.4) was used, transmitted light was acquired
521 using differential interference contrast (DIC), Fluorescein isothiocyanate (FITC) filter was
522 used to visualize GFP expressing bacteria and LysoTracker red fluorescence was acquired
523 using a Texas Red filter set.

524

525 **Phalloidin labeling**

526 J774 macrophages were seeded on glass coverslips and infected with GFP expressing bacteria
527 as described in the previous sections. For cytochalasin treatment, DMEM containing 2 μ M
528 cytochalasin D (Sigma) was added to the macrophages 1 hour before infection and maintained
529 during phagocytosis. After phagocytosis, the cells were maintained in 1 μ M cytochalasin D
530 till the end of the experiment. For untreated control, 0.2 % DMSO (solvent control) in DMEM
531 was added to the cells before and during phagocytosis. After phagocytosis, cells were
532 maintained in 0.1 % DMSO. After fixation with 4% paraformaldehyde (EMS, USA) in PBS
533 for 5 min, cells were washed once with PBS and permeabilized by adding 0.1% Triton X-100
534 for 1 min 30 sec. Cells were then washed once with PBS and incubated with 1 μ g/ml
535 Tetramethylrhodamine B isothiocyanate (TRITC)-labeled phalloidin (Sigma-Aldrich) in PBS
536 for 30 min in dark. Cells were washed twice with PBS and coverslips were mounted on glass
537 slides in Vectashield with DAPI (Vector Laboratories, Inc). The slides were examined using
538 an upright fluorescence microscope (Axioimager Z1, Zeiss) equipped with an Apotome 1 for
539 optical sectioning. A 63X Apochromat Objective (NA 1.4) was used and transmitted light was
540 acquired using DIC. FITC and Texas Red filters were used to visualize GFP expressing bacteria
541 and phalloidin respectively. Cell nuclei were visualized using DAPI filter. Images were
542 processed using ZEN software (Zeiss). Cells were counted manually, where infected cells
543 lacking the phalloidin stain were considered as lysed. Percentage of such lysed cells with

544 intracellular bacteria out of total number of infected cells was calculated and plotted for each
545 strain.

546 Strains containing pSBC6 plasmid (expressing *exsA* under the control of *tac* promoter) were
547 grown before infection in LB or in LB supplemented with 0.01 mM IPTG. Because these
548 strains did not harbor GFP producing plasmid, the number of total cells without phalloidin
549 label was counted and percentage out of total number of cells was plotted. The percent of
550 lysed cells for wild-type strain was similar to that found with GFP positive PAO1 strain.

551

552 **LDH cytotoxicity assay**

553 The cytotoxicity was assessed by release of LDH from infected J774 macrophages infected,
554 using the Pierce LDH cytotoxicity assay kit (Thermo Scientific). Macrophages were infected
555 for 2 hrs at an MOI of 10 as described above, except that cells were seeded in a 96 well plate
556 and extracellular bacteria were not removed. The assay was performed on 50 µl of the culture
557 supernatant according to manufacturer's instructions. LDH release was obtained by
558 subtracting the 680 nm absorbance value from 490 nm absorbance. The percentage of LDH
559 release was first normalized to that of the uninfected control and then calculated relatively to
560 that of uninfected cells lysed with Triton X-100, which was set at 100% LDH release.

561

562 **Trypan Blue exclusion test of cell viability**

563 The membrane impermeable dye Trypan Blue was used to quantify cell viability after
564 phagocytosis or after 2 hrs of gentamicin treatment following phagocytosis. Trypan Blue stain
565 (0.4%) was added in 1:1 ratio with PBS for 3 min at room temperature, replaced by PBS and
566 the cells were imaged using an optical microscope in bright field mode. Dead cells appear
567 blue as they take up the stain, in contrast to healthy cells that appear transparent because of

568 the exclusion of the dye. Cells were counted and the percentage of dead cells out of total cells
569 (blue + colorless) was calculated.

570

571 **RNA extraction and quantitative RT-PCR (qRT-PCR)**

572 For bacterial RNA extraction from infected J774, 6.5×10^6 macrophages were seeded into a
573 100 cm² tissue culture dish and infected at an MOI of 10 as described above. 1 hour after
574 phagocytosis, cells were washed three times with PBS, lysed with 0.1% Triton X100 and
575 pelleted by centrifugation at 13000 rpm for 10 min at 15°C. Bacteria were resuspended in 500
576 µl PBS and the non resuspended cellular debris was discarded. 900 µl of RNA protect reagent
577 (Qiagen) was added and incubated for 5 min. The sample was centrifuged at 13000 rpm for
578 10 min. Bacteria in the pellet were lysed with lyzozyme and RNA was prepared with RNEasy
579 kit (Qiagen). Superscript III reverse transcriptase (Invitrogen) was used for reverse
580 transcription. Controls without reverse transcriptase were done on each RNA sample to rule
581 out possible DNA contamination. Quantitative real-time PCR (q-RT-PCR) was performed
582 using a Light Cycler 480 SYBR Green I Master mix in a 480 Light Cycler instrument
583 (Roche). PCR conditions were as follows: 3 min denaturation at 98°C, 45 cycles of 98°C for 5
584 sec, 60°C for 10 sec and 72°C for 10 sec. The sequences of primers used for RT-PCR are
585 listed in Table S1.

586

587 **Cyclic di-GMP reporter assay**

588 The strains were transformed by electroporation with the plasmid pCdrA::*gfp* [34,38], which
589 expresses GFP under the control of the promoter of *cdrA*, a c-di-GMP responsive gene, and
590 carries a gentamicin resistance gene. Overnight cultures, grown in LB with 100 µg/ml
591 gentamicin, were subcultured in LB. These cultures were used to infect J774 cells seeded in a

592 96 well plate (Greiner, Flat-Bottom), containing 10^5 cells per well with an MOI of 20 after
593 normalizing the inoculum to their OD_{600} . After phagocytosis, DMEM containing 300 $\mu\text{g}/\text{ml}$
594 of amikacin, instead of gentamicin, was added to eliminate extracellular bacteria, as these
595 strains are resistant to gentamicin. At the required time point, Tecan fluorimeter (Spark 20M)
596 was used to measure fluorescence (excitation, 485 nm and emission, 520 nm) of cells at the Z
597 point where emission peak could be obtained in comparison to the blank. Fluorescence was
598 plotted for each strain in terms of arbitrary units (AU). CdrA activity of all strains was also
599 measured in liquid cultures under changing concentrations of magnesium. All strains, grown
600 overnight in LB, were diluted in LB and grown until OD_{600} of 0.6, washed in NCE medium
601 without magnesium and resuspended in NCE medium containing 1 mM, 10 μM or no
602 magnesium for 1 hour in 96 well plate (Greiner, Flat-Bottom). Their fluorescence (excitation,
603 485 nm and emission, 520 nm) and $OD_{600\text{nm}}$ was measured. Fluorescence ($AU_{520\text{nm}}$) was
604 normalized to $OD_{600\text{nm}}$ and plotted for each strain.

605

606 **CCF4 fluorometric assay to monitor the escape of *P. aeruginosa* in host cytosol**

607 The vacuole escape assay was adapted from the CCF4 FRET assay [43] using the CCF4-AM
608 LiveBlazer Loading Kit (Invitrogen) and an image-based quantification [62]. Briefly, J774
609 macrophages were seeded in 96 well plate (Greiner, Flat-Bottom), containing 5×10^4 cells per
610 well. Overnight bacterial cultures were subcultured in LB with 50 $\mu\text{g}/\text{ml}$ of ampicillin to
611 enhance the expression of beta-lactamase, present naturally in *P. aeruginosa*. Infection was
612 carried out as mentioned in the previous sections at the MOI of 10. After phagocytosis, the
613 cells were washed thrice with PBS to remove extracellular bacteria. 100 μl of HBSS buffer
614 containing 3 mM probenecid and gentamicin (400 $\mu\text{g}/\text{ml}$), was added in each well. The
615 substrate solution was prepared by mixing 6 μl of CCF4-AM (solution A), 60 μl of solution B
616 and 934 μl of solution C. 20 μl of the substrate solution was added to each well and the plate

617 was incubated in dark at 37 °C with 5% CO₂. After 2 hrs, the cells were imaged as described
618 in the Live Imaging section, using a 10X objective. FITC and DAPI channels were used to
619 visualize CCF4-FRET (Green) and loss of FRET (Blue) respectively. Each sample was taken
620 in triplicate and image acquisition was performed by automated random acquisition. Images
621 were analyzed by Cell Profiler software to calculate the number of blue and green cells. The
622 threshold for detection of blue signal by the software was normalized to uninfected control i.e.
623 no blue cells could be detected in the uninfected control. The percentage of blue cells,
624 representing the cells with cytosolic bacteria, out of total green cells was plotted. All strains
625 were tested for their ability to cleave CCF4 *in vitro*, before carrying out the vacuole rupture
626 assay. Overnight cultures grown in LB were subcultured at the ratio of 1:20 in LB with 100
627 µg/ml of ampicillin. After 2 hours of growth, the cultures were centrifuged and resuspended
628 in PBS. 100 µl of this was aliquoted in 96 well plate (Greiner, Flat-Bottom) and 20 µl of
629 CCF4 substrate solution (A+B+C) was added. Tecan fluorimeter (Spark 20M) was used to
630 measure fluorescence (excitation, 405 nm and emission, 450 nm) using PBS as blank. Blue
631 fluorescence (AU_{450nm}) was observed for all strains and none of the mutants exhibited
632 significantly lower value than the wild-type strain.

633

634 **Ethics statement**

635 Monocytes were issued from blood of anonymous donors obtained from the French blood
636 bank (Etablissement Français du Sang, approval EFS-OCPM n° 21PLER2018-0057).

637

638

639 **Acknowledgments**

640 We thank Sylvie Chevalier (Rouen), Ina Attrée and Sylvie Elsen (Grenoble) for providing
641 strains and plasmids, the Montpellier RIO Imaging microscopy platform for photonic
642 Microscopy and the Electron Microscopy facility of the University of Montpellier (MEA) for
643 sample preparation and transmission electron microscopy. We thank Bérengère Ize and Laila
644 Gannoun-Zaki for critical reading of the manuscript, Matteo Bonazzi and Fernande Siadous
645 for their expertise with the CCF4 assay, Chantal Soscia for testing ExoS secretion.

646

647

648 **References**

649

- 650 1. Silva MT (2012) Classical labeling of bacterial pathogens according to their lifestyle in the host:
651 inconsistencies and alternatives. *Front Microbiol* 3: 71.
- 652 2. Pujol C, Bliska JB (2005) Turning *Yersinia* pathogenesis outside in: subversion of macrophage
653 function by intracellular yersiniae. *Clin Immunol* 114: 216-226.
- 654 3. Kubica M, Guzik K, Koziel J, Zarebski M, Richter W, et al. (2008) A potential new pathway for
655 *Staphylococcus aureus* dissemination: the silent survival of *S. aureus* phagocytosed by human
656 monocyte-derived macrophages. *PLoS One* 3: e1409.
- 657 4. Garzoni C, Kelley WL (2009) *Staphylococcus aureus*: new evidence for intracellular persistence.
658 *Trends Microbiol* 17: 59-65.
- 659 5. Flannagan RS, Heit B, Heinrichs DE (2016) Intracellular replication of *Staphylococcus aureus* in
660 mature phagolysosomes in macrophages precedes host cell death, and bacterial escape and
661 dissemination. *Cell Microbiol* 18: 514-535.
- 662 6. Jubrail J, Morris P, Bewley MA, Stoneham S, Johnston SA, et al. (2016) Inability to sustain
663 intraphagolysosomal killing of *Staphylococcus aureus* predisposes to bacterial persistence in
664 macrophages. *Cell Microbiol* 18: 80-96.
- 665 7. Ercoli G, Fernandes VE, Chung WY, Wanford JJ, Thomson S, et al. (2018) Intracellular replication of
666 *Streptococcus pneumoniae* inside splenic macrophages serves as a reservoir for septicemia.
667 *Nat Microbiol*.
- 668 8. Klockgether J, Tummler B (2017) Recent advances in understanding *Pseudomonas aeruginosa* as a
669 pathogen. *F1000Res* 6: 1261.
- 670 9. Engel J, Balachandran P (2009) Role of *Pseudomonas aeruginosa* type III effectors in disease. *Curr*
671 *Opin Microbiol* 12: 61-66.
- 672 10. Hauser AR (2009) The type III secretion system of *Pseudomonas aeruginosa*: infection by
673 injection. *Nat Rev Microbiol* 7: 654-665.

- 674 11. Feltman H, Schulert G, Khan S, Jain M, Peterson L, et al. (2001) Prevalence of type III secretion
675 genes in clinical and environmental isolates of *Pseudomonas aeruginosa*. *Microbiology* 147:
676 2659-2669.
- 677 12. Garcia-Medina R, Dunne WM, Singh PK, Brody SL (2005) *Pseudomonas aeruginosa* acquires
678 biofilm-like properties within airway epithelial cells. *Infect Immun* 73: 8298-8305.
- 679 13. Sana TG, Hachani A, Bucior I, Soscia C, Garvis S, et al. (2012) The second type VI secretion system
680 of *Pseudomonas aeruginosa* strain PAO1 is regulated by quorum sensing and Fur and
681 modulates internalization in epithelial cells. *J Biol Chem* 287: 27095-27105.
- 682 14. Mittal R, Grati M, Gerring R, Blackwelder P, Yan D, et al. (2014) In vitro interaction of
683 *Pseudomonas aeruginosa* with human middle ear epithelial cells. *PLoS One* 9: e91885.
- 684 15. Kazmierczak BI, Jou TS, Mostov K, Engel JN (2001) Rho GTPase activity modulates *Pseudomonas*
685 *aeruginosa* internalization by epithelial cells. *Cell Microbiol* 3: 85-98.
- 686 16. Angus AA, Lee AA, Augustin DK, Lee EJ, Evans DJ, et al. (2008) *Pseudomonas aeruginosa* induces
687 membrane blebs in epithelial cells, which are utilized as a niche for intracellular replication
688 and motility. *Infect Immun* 76: 1992-2001.
- 689 17. Kroken AR, Chen CK, Evans DJ, Yahr TL, Fleiszig SMJ (2018) The Impact of ExoS on *Pseudomonas*
690 *aeruginosa* Internalization by Epithelial Cells Is Independent of fleQ and Correlates with
691 Bistability of Type Three Secretion System Gene Expression. *MBio* 9.
- 692 18. Angus AA, Evans DJ, Barbieri JT, Fleiszig SM (2010) The ADP-ribosylation domain of *Pseudomonas*
693 *aeruginosa* ExoS is required for membrane bleb niche formation and bacterial survival within
694 epithelial cells. *Infect Immun* 78: 4500-4510.
- 695 19. Heimer SR, Evans DJ, Stern ME, Barbieri JT, Yahr T, et al. (2013) *Pseudomonas aeruginosa* utilizes
696 the type III secreted toxin ExoS to avoid acidified compartments within epithelial cells. *PLoS*
697 *One* 8: e73111.
- 698 20. Lovewell RR, Patankar YR, Berwin B (2014) Mechanisms of phagocytosis and host clearance of
699 *Pseudomonas aeruginosa*. *Am J Physiol Lung Cell Mol Physiol* 306: L591-603.
- 700 21. Brannon MK, Davis JM, Mathias JR, Hall CJ, Emerson JC, et al. (2009) *Pseudomonas aeruginosa*
701 Type III secretion system interacts with phagocytes to modulate systemic infection of
702 zebrafish embryos. *Cell Microbiol* 11: 755-768.
- 703 22. Kumar SS, Tandberg JI, Penesyan A, Elbourne LDH, Suarez-Bosche N, et al. (2018) Dual
704 Transcriptomics of Host-Pathogen Interaction of Cystic Fibrosis Isolate *Pseudomonas*
705 *aeruginosa* PASS1 With Zebrafish. *Front Cell Infect Microbiol* 8: 406.
- 706 23. Schmiedl A, Kerber-Momot T, Munder A, Pabst R, Tschernig T (2010) Bacterial distribution in lung
707 parenchyma early after pulmonary infection with *Pseudomonas aeruginosa*. *Cell Tissue Res*
708 342: 67-73.
- 709 24. Buyck JM, Tulkens PM, Van Bambeke F (2013) Pharmacodynamic evaluation of the intracellular
710 activity of antibiotics towards *Pseudomonas aeruginosa* PAO1 in a model of THP-1 human
711 monocytes. *Antimicrob Agents Chemother* 57: 2310-2318.
- 712 25. Belon C, Soscia C, Bernut A, Laubier A, Bleves S, et al. (2015) A Macrophage Subversion Factor Is
713 Shared by Intracellular and Extracellular Pathogens. *PLoS Pathog* 11: e1004969.
- 714 26. Mittal R, Lisi CV, Kumari H, Grati M, Blackwelder P, et al. (2016) Otopathogenic *Pseudomonas*
715 *aeruginosa* Enters and Survives Inside Macrophages. *Front Microbiol* 7: 1828.
- 716 27. Bernut A, Belon C, Soscia C, Bleves S, Blanc-Potard AB (2015) Intracellular phase for an
717 extracellular bacterial pathogen: MgtC shows the way. *Microb Cell* 2: 353-355.
- 718 28. Lee EJ, Pontes MH, Groisman EA (2013) A bacterial virulence protein promotes pathogenicity by
719 inhibiting the bacterium's own F1Fo ATP synthase. *Cell* 154: 146-156.
- 720 29. Pontes MH, Lee EJ, Choi J, Groisman EA (2015) *Salmonella* promotes virulence by repressing
721 cellulose production. *Proc Natl Acad Sci U S A* 112: 5183-5188.
- 722 30. Alix E, Blanc-Potard AB (2007) MgtC: a key player in intramacrophage survival. *Trends Microbiol*
723 15: 252-256.
- 724 31. Belon C, Blanc-Potard AB (2016) Intramacrophage Survival for Extracellular Bacterial Pathogens:
725 MgtC As a Key Adaptive Factor. *Front Cell Infect Microbiol* 6: 52.

- 726 32. Fito-Boncompte L, Chapalain A, Bouffartigues E, Chaker H, Lesouhaitier O, et al. (2011) Full
727 virulence of *Pseudomonas aeruginosa* requires OprF. *Infect Immun* 79: 1176-1186.
- 728 33. Chevalier S, Bouffartigues E, Bodilis J, Maillot O, Lesouhaitier O, et al. (2017) Structure, function
729 and regulation of *Pseudomonas aeruginosa* porins. *FEMS Microbiol Rev* 41: 698-722.
- 730 34. Bouffartigues E, Moscoso JA, Duchesne R, Rosay T, Fito-Boncompte L, et al. (2015) The absence of
731 the *Pseudomonas aeruginosa* OprF protein leads to increased biofilm formation through
732 variation in c-di-GMP level. *Front Microbiol* 6: 630.
- 733 35. Ince D, Sutterwala FS, Yahr TL (2015) Secretion of Flagellar Proteins by the *Pseudomonas*
734 *aeruginosa* Type III Secretion-Injectisome System. *J Bacteriol* 197: 2003-2011.
- 735 36. Soscia C, Hachani A, Bernadac A, Filloux A, Bleves S (2007) Cross talk between type III secretion
736 and flagellar assembly systems in *Pseudomonas aeruginosa*. *J Bacteriol* 189: 3124-3132.
- 737 37. Moscoso JA, Mikkelsen H, Heeb S, Williams P, Filloux A (2011) The *Pseudomonas aeruginosa*
738 sensor RetS switches type III and type VI secretion via c-di-GMP signalling. *Environ Microbiol*
739 13: 3128-3138.
- 740 38. Rybtke MT, Borlee BR, Murakami K, Irie Y, Hentzer M, et al. (2012) Fluorescence-based reporter
741 for gauging cyclic di-GMP levels in *Pseudomonas aeruginosa*. *Appl Environ Microbiol* 78:
742 5060-5069.
- 743 39. Coburn J, Frank DW (1999) Macrophages and epithelial cells respond differently to the
744 *Pseudomonas aeruginosa* type III secretion system. *Infect Immun* 67: 3151-3154.
- 745 40. Franchi L, Stoolman J, Kanneganti TD, Verma A, Ramphal R, et al. (2007) Critical role for Ipaf in
746 *Pseudomonas aeruginosa*-induced caspase-1 activation. *Eur J Immunol* 37: 3030-3039.
- 747 41. Galle M, Schotte P, Haegman M, Wullaert A, Yang HJ, et al. (2008) The *Pseudomonas aeruginosa*
748 Type III secretion system plays a dual role in the regulation of caspase-1 mediated IL-1 β
749 maturation. *J Cell Mol Med* 12: 1767-1776.
- 750 42. Huber P, Bouillot S, Elsen S, Attree I (2014) Sequential inactivation of Rho GTPases and Lim kinase
751 by *Pseudomonas aeruginosa* toxins ExoS and ExoT leads to endothelial monolayer
752 breakdown. *Cell Mol Life Sci* 71: 1927-1941.
- 753 43. Keller C, Mellouk N, Danckaert A, Simeone R, Brosch R, et al. (2013) Single cell measurements of
754 vacuolar rupture caused by intracellular pathogens. *J Vis Exp*: e50116.
- 755 44. Tsutsumi Y, Tomita H, Tanimoto K (2013) Identification of novel genes responsible for
756 overexpression of ampC in *Pseudomonas aeruginosa* PAO1. *Antimicrob Agents Chemother*
757 57: 5987-5993.
- 758 45. Hritonenko V, Evans DJ, Fleiszig SM (2012) Translocon-independent intracellular replication by
759 *Pseudomonas aeruginosa* requires the ADP-ribosylation domain of ExoS. *Microbes Infect* 14:
760 1366-1373.
- 761 46. Landeta C, Boyd D, Beckwith J (2018) Disulfide bond formation in prokaryotes. *Nat Microbiol* 3:
762 270-280.
- 763 47. Vareechon C, Zmina SE, Karmakar M, Pearlman E, Rietsch A (2017) *Pseudomonas aeruginosa*
764 Effector ExoS Inhibits ROS Production in Human Neutrophils. *Cell Host Microbe* 21: 611-618
765 e615.
- 766 48. Hauser AR, Engel JN (1999) *Pseudomonas aeruginosa* induces type-III-secretion-mediated
767 apoptosis of macrophages and epithelial cells. *Infect Immun* 67: 5530-5537.
- 768 49. Dacheux D, Toussaint B, Richard M, Brochier G, Croize J, et al. (2000) *Pseudomonas aeruginosa*
769 cystic fibrosis isolates induce rapid, type III secretion-dependent, but ExoU-independent,
770 oncosis of macrophages and polymorphonuclear neutrophils. *Infect Immun* 68: 2916-2924.
- 771 50. Vance RE, Rietsch A, Mekalanos JJ (2005) Role of the type III secreted exoenzymes S, T, and Y in
772 systemic spread of *Pseudomonas aeruginosa* PAO1 in vivo. *Infect Immun* 73: 1706-1713.
- 773 51. Sutterwala FS, Mijares LA, Li L, Ogura Y, Kazmierczak BI, et al. (2007) Immune recognition of
774 *Pseudomonas aeruginosa* mediated by the IPAF/NLRC4 inflammasome. *J Exp Med* 204: 3235-
775 3245.

- 776 52. Balakrishnan A, Karki R, Berwin B, Yamamoto M, Kanneganti TD (2018) Guanylate binding
777 proteins facilitate caspase-11-dependent pyroptosis in response to type 3 secretion system-
778 negative *Pseudomonas aeruginosa*. *Cell Death Discov* 5: 3.
- 779 53. Kaminski A, Gupta KH, Goldufsky JW, Lee HW, Gupta V, et al. (2018) *Pseudomonas aeruginosa*
780 ExoS Induces Intrinsic Apoptosis in Target Host Cells in a Manner That is Dependent on its
781 GAP Domain Activity. *Sci Rep* 8: 14047.
- 782 54. Pederson KJ, Vallis AJ, Aktories K, Frank DW, Barbieri JT (1999) The amino-terminal domain of
783 *Pseudomonas aeruginosa* ExoS disrupts actin filaments via small-molecular-weight GTP-
784 binding proteins. *Mol Microbiol* 32: 393-401.
- 785 55. Wood SJ, Goldufsky JW, Bello D, Masood S, Shafikhani SH (2015) *Pseudomonas aeruginosa* ExoT
786 Induces Mitochondrial Apoptosis in Target Host Cells in a Manner That Depends on Its
787 GTPase-activating Protein (GAP) Domain Activity. *J Biol Chem* 290: 29063-29073.
- 788 56. Sawa T, Shimizu M, Moriyama K, Wiener-Kronish JP (2014) Association between *Pseudomonas*
789 *aeruginosa* type III secretion, antibiotic resistance, and clinical outcome: a review. *Crit Care*
790 18: 668.
- 791 57. Munzenmayer L, Geiger T, Daiber E, Schulte B, Autenrieth SE, et al. (2016) Influence of Sae-
792 regulated and Agr-regulated factors on the escape of *Staphylococcus aureus* from human
793 macrophages. *Cell Microbiol* 18: 1172-1183.
- 794 58. Rang C, Alix E, Felix C, Heitz A, Tasse L, et al. (2007) Dual role of the MgtC virulence factor in host
795 and non-host environments. *Mol Microbiol* 63: 605-622.
- 796 59. Nivens DE, Ohman DE, Williams J, Franklin MJ (2001) Role of alginate and its O acetylation in
797 formation of *Pseudomonas aeruginosa* microcolonies and biofilms. *J Bacteriol* 183: 1047-
798 1057.
- 799 60. Bessoles S, Dudal S, Besra GS, Sanchez F, Lafont V (2009) Human CD4+ invariant NKT cells are
800 involved in antibacterial immunity against *Brucella suis* through CD1d-dependent but CD4-
801 independent mechanisms. *Eur J Immunol* 39: 1025-1035.
- 802 61. Gannoun-Zaki L, Alibaud L, Carrere-Kremer S, Kremer L, Blanc-Potard AB (2013) Overexpression
803 of the KdpF membrane peptide in *Mycobacterium bovis* BCG results in reduced
804 intramacrophage growth and altered cording morphology. *PLoS One* 8: e60379.
- 805 62. Martinez E, Allombert J, Cantet F, Lakhani A, Yandrapalli N, et al. (2016) *Coxiella burnetii* effector
806 CvpB modulates phosphoinositide metabolism for optimal vacuole development. *Proc Natl*
807 *Acad Sci U S A* 113: E3260-3269.

808

809

810

811 **Figure legends**

812

813 **Fig 1. Live imaging of macrophages infected with *P. aeruginosa*.** J774 macrophages were
814 infected with PAO1 wild-type (WT) strain expressing GFP. Time lapse imaging was started at
815 1.5 hrs post-phagocytosis. Cells were maintained in DMEM supplemented with gentamicin at
816 37°C and 5% CO₂ throughout imaging. White arrows point at the cells that harbor
817 intracellular bacteria and undergo lysis between 1.5 hrs and 3 hrs post-phagocytosis. Black
818 arrow shows an uninfected and unlyed cell. Scale bar is equivalent to 10 μm.

819

820 **Fig 2. Transmission electron micrographs (TEM) of *P. aeruginosa* within macrophages.**
821 J774 macrophages were infected with *P. aeruginosa* for 30 min (A) or 3 hrs (B and C) and
822 subjected to TEM (left panels). Black rectangles show intracellular bacteria that are shown at
823 higher magnification in the right panels. A. At early time after phagocytosis, most of bacteria
824 were found inside membrane bound vacuoles (white arrows). B. At later time, some bacteria
825 can be observed in the cytoplasm with no surrounding membrane suggesting disruption of the
826 vacuole membrane (black arrows). The infected macrophage in panel B shows an abnormal
827 morphology, with highly condensed chromatin and membrane blebbing, but no pseudopodia.
828 C. At later time, bacteria can also be found in vacuole partially or totally filled with
829 heterogeneous electron dense material (white arrows), suggesting that the vacuole has fused
830 with lysosomes. The infected macrophage shown in panel C appears normal.

831

832 **Fig 3. Visualization (A) and quantification (B) of lysed infected cells upon phalloidin**
833 **labeling.** GFP expressing PAO1 WT, Δ *mgtC* and Δ *oprF* strains were used for infecting J774
834 macrophages. Gentamicin was added after phagocytosis and cells were fixed at 2 hrs post-
835 phagocytosis, stained with phalloidin and imaged with fluorescent microscope. DAPI was

836 used to stain the nucleus. Cells that have intracellular bacteria, but lack the phalloidin cortical
837 label were considered as lysed by intracellular bacteria (shown by arrows). Scale bar is
838 equivalent to 10 μ m. After imaging, infected cells were counted and percentage of lysed cells
839 with intracellular bacteria out of total number of cells was plotted for each strain. Error bars
840 correspond to standard errors from three independent experiments. At least 200 cells were
841 counted per strain. The asterisks indicate *P* values (One way ANOVA, where all strains were
842 compared to WT using Dunnet's multiple comparison post-test, **P* <0.05 and ****P* <0.001),
843 showing statistical significance with respect to WT.

844

845 **Fig 4. Expression of T3SS genes in *P. aeruginosa* strains residing in J774 macrophages.**

846 J774 macrophages were infected with PAO1 WT, Δ *mgtC* and Δ *oprF* strains. After
847 phagocytosis, cells were maintained in DMEM supplemented with gentamicin. RNA was
848 extracted from bacteria isolated from infected macrophages 1 hr after phagocytosis. The level
849 of *exoS*, *pcrV* and *fliC* transcripts relative to those of the house-keeping gene *rpoD* was
850 measured by qRT-PCR and plotted on the Y-axis. Error bars correspond to standard errors
851 from at least three independent experiments. The asterisks indicate *P* values (One way
852 ANOVA, where all strains were compared to WT using Dunnet's multiple comparison post-
853 test, **P* <0.05, ***P* <0.01, ****P* <0.001 and ns = *P* >0.05 or non-significant), showing
854 statistical significance with respect to WT.

855

856 **Fig 5. Measurement of c-di-GMP level in Δ *mgtC* and Δ *oprF* mutants.** PAO1 WT, Δ *mgtC*

857 and Δ *oprF* harboring reporter plasmid pCdrA::*gfp*, which expresses GFP under the control of
858 the promoter of c-di-GMP responsive gene *cdrA* (A), were used to infect J774 cells and
859 fluorescence was measured (B). After phagocytosis, DMEM containing 300 μ g/ml of

860 amikacin was added to eliminate extracellular bacteria. Fluorescence (excitation, 485 nm and
861 emission, 520 nm) was measured 1 hour after phagocytosis and plotted as arbitrary units
862 (AU). Error bars correspond to standard errors from four independent experiments. The
863 asterisks indicate *P* values (One way ANOVA, where all strains were compared to WT using
864 Dunnet's multiple comparison post-test, **P* <0.05 and ****P* <0.001), showing statistical
865 significance with respect to WT. C. PAO1 WT, Δ *mgtC* and Δ *oprF* harboring reporter plasmid
866 pCdrA::*gfp*, were grown in NCE medium with varying concentration of Mg²⁺. After 1 hour of
867 growth, fluorescence (excitation, 485 nm and emission, 520 nm) of the culture was measured
868 along with its O.D_{600nm}. The fluorescence was plotted as arbitrary units (AU_{520nm}) after
869 normalizing with O.D_{600nm} (C). Error bars correspond to standard errors from three
870 independent experiments. The asterisks indicate *P* values showing statistical significance with
871 respect to WT in the respective condition, using Student's t test (ns = *P* >0.05, **P* <0.05, ***P*
872 <0.01 and ****P* <0.001).

873

874 **Fig 6. Assessment of role of T3SS and its effectors in cell lysis induced by intracellular**
875 **PAO1.** J774 macrophages were infected with GFP expressing strains as indicated. After
876 phagocytosis, cells were maintained in DMEM supplemented with gentamicin. Cells were
877 imaged 2 hrs post-phagocytosis after staining with phalloidin (A). Scale bar is equivalent to
878 10 μ m. Lysis was quantified (B & C) by counting infected cells lacking cortical labeling
879 (indicated by arrows). Percentage of lysed cells with intracellular bacteria out of total number
880 of cells was plotted. Error bars correspond to standard errors from at least three independent
881 experiments. At least 200 cells were counted per strain. The asterisks indicate *P* values (One
882 way ANOVA, where all strains were compared to WT using Dunnet's multiple comparison
883 test, ****P* <0.001), showing statistical significance with respect to WT.

884

885 **Fig 7. Visualization and quantification of lysis of infected primary human macrophages**
886 **driven intracellularly by *P. aeruginosa* strains.** HMDMs were infected with GFP
887 expressing PAO1 WT, $\Delta oprF$, and \DeltapscN strains. After phagocytosis, cells were maintained
888 in RPMI supplemented with gentamicin. Cells were imaged 2 hrs post-phagocytosis after
889 staining with phalloidin (A) and lysis was quantified (B) by counting infected cells lacking
890 cortical labeling (indicated by arrows). Scale bar is equivalent to 10 μ m. Percentage of lysed
891 cells with intracellular bacteria out of total number of cells was plotted. Error bars correspond
892 to standard errors from two independent experiments. At least 200 cells were counted per
893 strain. The asterisks indicate *P* values (One way ANOVA, where all strains were compared to
894 WT using Bonferroni's multiple comparison test, $***P < 0.001$), showing statistical
895 significance with respect to WT.

896

897 **Fig 8. Assessment of access of *P. aeruginosa* to host cytosol using phagosome escape**
898 **assay.** J774 macrophages were infected with PAO1 WT, $\Delta mgtC$, $\Delta oprF$ and \DeltapscN strains.
899 After phagocytosis, cells were stained with CCF4-AM in presence of gentamicin. 2 hours
900 post-phagocytosis, the cells were imaged with 10X objective using FITC and DAPI channels.
901 Upon escape of bacteria from phagosome to the cytosol, the CCF4-AM FRET is lost,
902 producing blue color. **A.** Representative pictures are shown with the following channels: Total
903 cell population is shown in merged green and blue cells, whereas cells with cleaved CCF4
904 probe are shown in blue in the lower panel. Scale bar is equivalent to 50 μ m. **B.** Images were
905 analyzed and quantified by Cell Profiler software to calculate the percentage of blue cells out
906 of total green cells. At least 200 cells were counted per strain. Error bars correspond to
907 standard errors from three independent experiments. The asterisks indicate *P* values (One way
908 ANOVA, where all strains were compared to WT using Dunnet's multiple comparison post-
909 test, $**P < 0.01$ and $***P < 0.001$), showing statistical significance with respect to WT. **C.**

910 Electron micrograph showing a disrupted vacuole membrane (white arrows) in a macrophage
911 infected with PAO1 strain. The right panel shows higher magnification of the black square in
912 the left panel.

913

914 **Fig 9. Model for intramacrophage fate of *P. aeruginosa*.** Phagocytosed *P. aeruginosa*
915 PAO1 first resides in a vacuole, before escaping the phagosome and promoting macrophage
916 lysis. This cell lysis driven by intracellular *P. aeruginosa* involves the T3SS and more
917 specifically ExoS. MgtC and OprF act positively on the expression of T3SS, possibly by
918 reducing c-di-GMP level, a negative regulator of T3SS expression. Thereby T3SS and its
919 effector ExoS play a role in phagosomal escape and cell lysis. Further work will be required
920 to address secretion of ExoS from intracellularly expressed T3SS as well as identify host-
921 targets.

922

923

924 **Supporting Information**

925 **S1 Fig. Live imaging of macrophages infected with *P. aeruginosa*.** J774 macrophages were
926 infected with PAO1 wild-type strain expressing GFP. Time lapse imaging was started at 1.5
927 hrs post-phagocytosis. Cells were maintained in DMEM supplemented with gentamicin, at 37
928 °C and 5% CO₂ throughout imaging. White arrows point at infected cells that undergo lysis,
929 whereas black arrows indicate uninfected cells that do not lyse. Images were taken between
930 1.5 hrs and 3 hrs post-phagocytosis as shown on the panels. Scale bar is equivalent to 10 μm.

931

932 **S2 Fig. Live imaging of primary human macrophages infected with *P. aeruginosa*.**
933 HMDMs were infected with PAO1 wild-type (WT) strain expressing GFP. Time lapse
934 imaging was started at 1.5 hrs post-phagocytosis. Cells were maintained in RPMI
935 supplemented with gentamicin at 37°C and 5% CO₂ throughout imaging. White arrows point
936 at the cells that harbor intracellular bacteria and undergo lysis between 1.5 hrs and 3 hrs post-
937 phagocytosis. Black arrow shows an uninfected and unlysed cell. Scale bar is equivalent to 20
938 μm.

939

940 **S3 Fig. Colocalization of *P. aeruginosa* with a probe that labels acidic compartments.**
941 J774 macrophages were infected with PAO1 expressing GFP. After 2.5 hrs of gentamicin
942 treatment, infected J774 cells were incubated with LysoTracker for 10 min, a red fluorescent
943 weak base that accumulates in acidic compartments. Cells were then fixed and imaged with
944 fluorescence microscope. (A) The image shows individual panels for Differential Interference
945 Contrast (DIC), lysosomal compartment (red), bacteria expressing GFP (green), the nucleus
946 (blue) and merged image of all channels. The solid arrow shows colocalization of bacteria

947 with lysotracker and dashed arrow shows non-colocalization. Scale bar is equivalent to 5 μm .
948 (B) 3D-reconstructed image of the same area of (A).

949

950 **S4 Fig. Visualization (A) and quantification (B) of lysed infected cells upon cytochalasin**
951 **D treatment.** GFP expressing PAO1 used for infecting J774 macrophages. DMEM
952 containing 2 μM cytochalasin D was added to the macrophages 1 hour before infection and
953 maintained during phagocytosis. After phagocytosis, cells were maintained in 1 μM
954 cytochalasin D in DMEM supplemented with gentamicin till the end of the experiment. 0.2 %
955 DMSO in DMEM was added to the cells as solvent control before and during phagocytosis.
956 After phagocytosis, cells were maintained in 0.1 % DMSO in DMEM with gentamicin, fixed
957 2 hrs post-phagocytosis, stained with phalloidin and imaged with fluorescent microscope.
958 DAPI was used to stain the nucleus. Cells that have intracellular bacteria, but lack the
959 phalloidin cortical label, were considered as lysed by intracellular bacteria (shown by arrows).
960 Scale bar is equivalent to 10 μm . Percentage of lysed cells with intracellular bacteria out of
961 total number of cells was plotted. Error bars correspond to standard errors from two
962 independent experiments. At least 200 cells were counted per strain. The asterisks indicate *P*
963 values (Student's t-test, *****P* < 0.01**), showing statistical significance with respect to DMSO
964 control.

965

966 **S5 Fig. Quantification of dying cells infected with *P. aeruginosa* strains overexpressing**
967 ***exsA*.** PAO1 WT, ΔoprF , PAO1 WT + *pexsA* and ΔoprF + *pexsA* strains were used for
968 infecting J774 macrophages. Expression of *exsA* was induced by adding 0.01 mM IPTG for
969 the strains PAO1 WT + *pexsA* and ΔoprF + *pexsA*. Gentamicin was added after phagocytosis
970 and cells were fixed at 2 hrs post-phagocytosis, stained with phalloidin and imaged with

971 fluorescent microscope. DAPI was used to stain the nucleus. Cells that lack the phalloidin
972 cortical label were considered as lysed by intracellular bacteria. After imaging, percentage of
973 lysed cells out of total number of cells was plotted for each strain. Error bars correspond to
974 standard errors from at least three independent experiments. At least 200 cells were counted
975 per strain. The asterisks indicate *P* values (One way ANOVA, where all strains were
976 compared to each other using Bonferroni's multiple comparison post-test, $**P < 0.01$ and $ns =$
977 $P > 0.05$), showing statistical significance with respect to WT.

978

979 **S6 Fig. Quantification of cell lysis driven by extracellular bacteria.** Release of LDH was
980 measured from J774 macrophages infected for 2 hrs with PAO1 WT, $\Delta pscN$, $\Delta exoS$ and
981 $\Delta exoSTY$ mutant strains to quantify the cytotoxicity. The percentage of LDH release was
982 calculated relatively to that of total uninfected cells lysed with Triton X-100, which was set at
983 100% LDH release. Error bars correspond to standard errors (SE) from at least four
984 independent experiments. The asterisks indicate *P* values (One way ANOVA, where all
985 strains were compared to WT using Dunnet's multiple comparison post-test, $**P < 0.01$),
986 showing statistical significance with respect to WT.

987

988 **S7 Fig. Quantification of lysed cells by staining with Trypan Blue.** J774 macrophages
989 were infected with the strains as indicated. After phagocytosis, cells were maintained in
990 DMEM supplemented with gentamicin. Cells were stained with trypan blue at (A) 30 min or
991 (B) 2 hrs post-phagocytosis and imaged. Lysed cells were quantified by counting cells stained
992 with trypan blue and the percentage of lysed cells out of total number of cells was plotted.
993 Error bars correspond to standard errors from at least three independent experiments. At least
994 400 cells were counted per strain. The asterisks indicate *P* values (One way ANOVA, where

995 all strains were compared to WT using Dunnet's multiple comparison test, * $P < 0.05$, ** P
996 < 0.01 and *** $P < 0.001$), showing statistical significance with respect to WT.

997

998 **S8 Fig. Assessment of β -lactamase activity in liquid culture.** PAO1 WT, $\Delta mgtC$, $\Delta oprF$,
999 $\Delta pscN$, $\Delta exoS$ and $\Delta exoSTY$ strains grown in presence of ampicillin, were incubated with
1000 CCF4-AM for 1 hour. The blue fluorescence generated as a result of loss of FRET of CCF4
1001 was measured (excitation, 420 nm and emission, 450 nm) and plotted as arbitrary units (AU).
1002 Error bars correspond to standard errors from four independent experiments. All strains were
1003 compared to WT using One way ANOVA, Dunnet's multiple comparison post-test. No
1004 significant difference was found between the mutant strains and WT.

1005

1006 **S9 Fig. Phagosome escape assay of T3SS mutants.** J774 macrophages were infected with
1007 PAO1 WT, $\Delta pscN$, $\Delta exoS$ and $\Delta exoSTY$ strains. After phagocytosis, cells were stained with
1008 CCF4-AM in presence of gentamicin. 2 hours post-phagocytosis, the cells were imaged with
1009 10X objective using FITC and DAPI channels. Upon escape of bacteria from phagosome to
1010 the cytosol, the CCF4-AM FRET is lost, producing blue color. Images were analyzed and
1011 quantified by Cell Profiler software to calculate the percentage of blue cells out of total green
1012 cells. At least 200 cells were counted per strain. Error bars correspond to standard errors from
1013 four independent experiments. The asterisks indicate P values (One way ANOVA, where all
1014 strains were compared to WT using Dunnet's multiple comparison post-test, * $P < 0.05$),
1015 showing statistical significance with respect to WT.

1016

1017 **S10 Fig. Comparison of secreted protein profiles and ExoS production under T3SS-**
1018 **inducing conditions in two PAO1 strains.** Immunodetection of the ExoS effector in culture

1019 supernatant of PAO1 (S. Bleves) and PAO1 H103 (isogenic WT strain for *oprF* mutant)
1020 grown in exponential phase at 37°C under T3SS-inducing ($- \text{Ca}^{2+}$) or non-inducing ($+ \text{Ca}^{2+}$)
1021 conditions. The bacterial culture equivalent of 0.1 or 1 OD_{600} unit was loaded on an SDS gel
1022 containing 10% polyacrylamide. As control, cellular fraction (equivalent of 0.1 OD_{600} unit
1023 was loaded). Upper panels show Western blot using anti-ExoS antibodies (Soscia et al., 2007;
1024 doi: [10.1128/JB.01677-06](https://doi.org/10.1128/JB.01677-06)) and lower panels show Coomassie stained gels.

1025

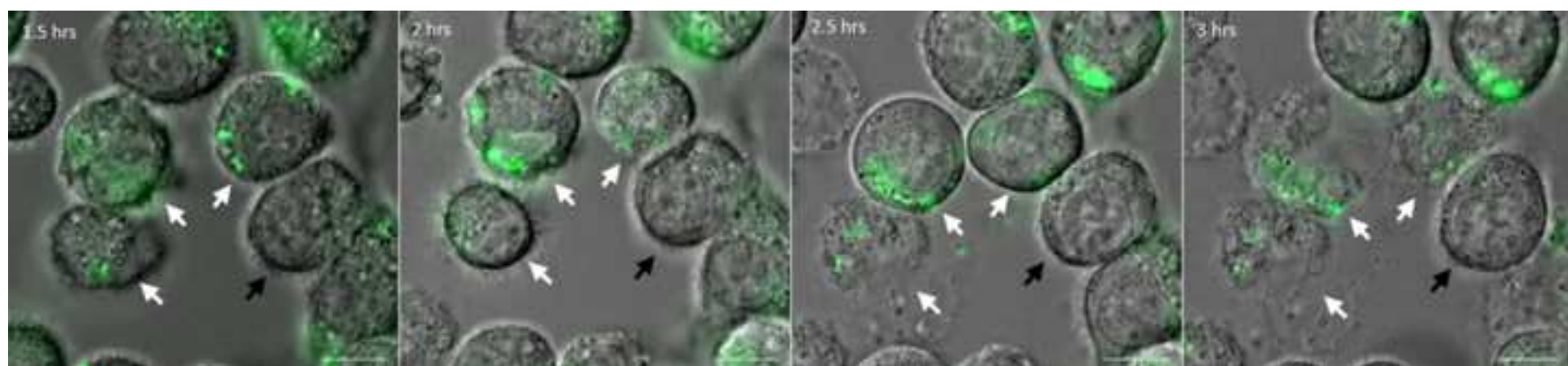
1026

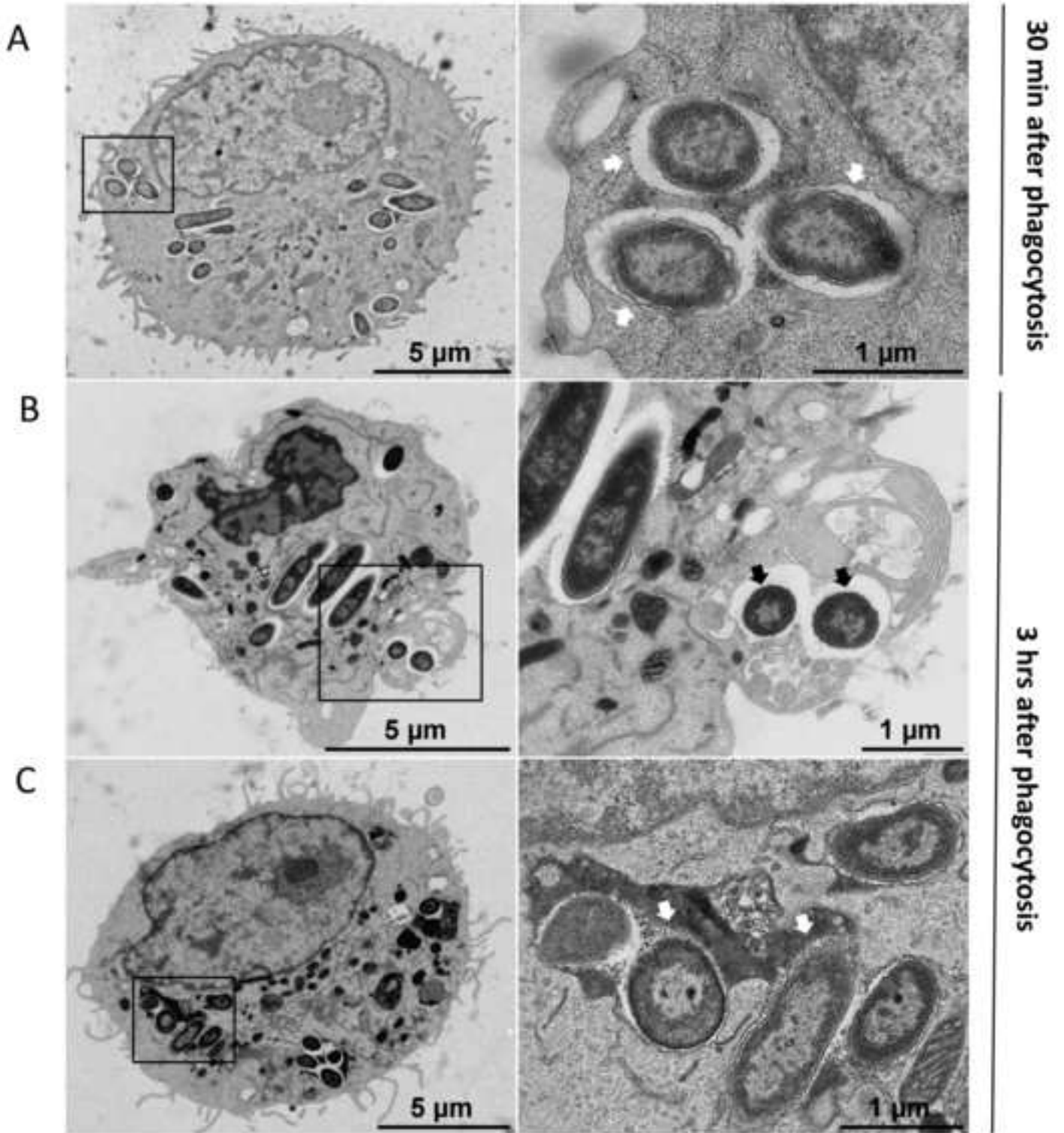
1027 **S1 Movie. Live microscopy movie imaging cell lysis in real time.** J774 macrophages were
1028 infected with PAO1 WT strain expressing GFP. Cells were maintained in DMEM
1029 supplemented with gentamicin, at 37 °C and 5% CO_2 throughout imaging. Imaging was
1030 started at 3 hrs post-phagocytosis and continued for 10 min with interval of 30 sec between
1031 frames. The time frame is displayed in the movie in the format of minutes:seconds.milli
1032 seconds. The movie shows quick lysis of macrophages harboring intracellular bacteria
1033 occurring within a minute.

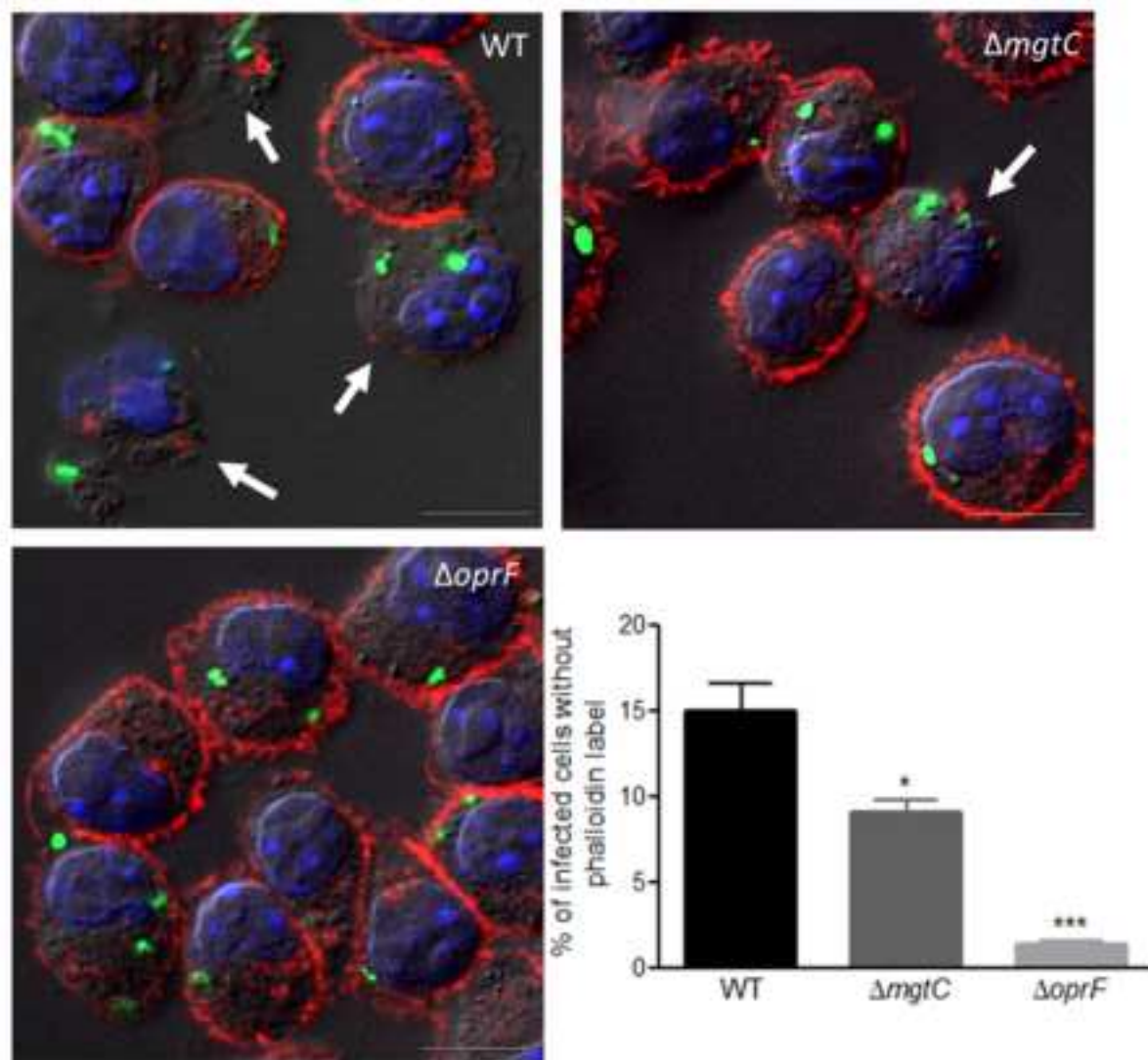
1034

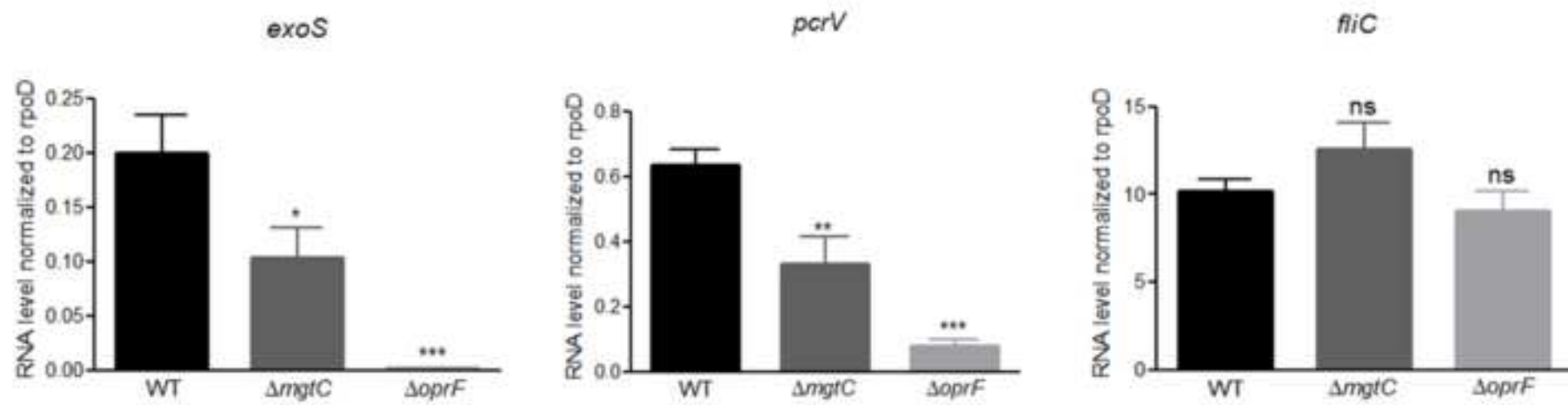
1035 **S1 Table. List of primers used for RT-PCR.**

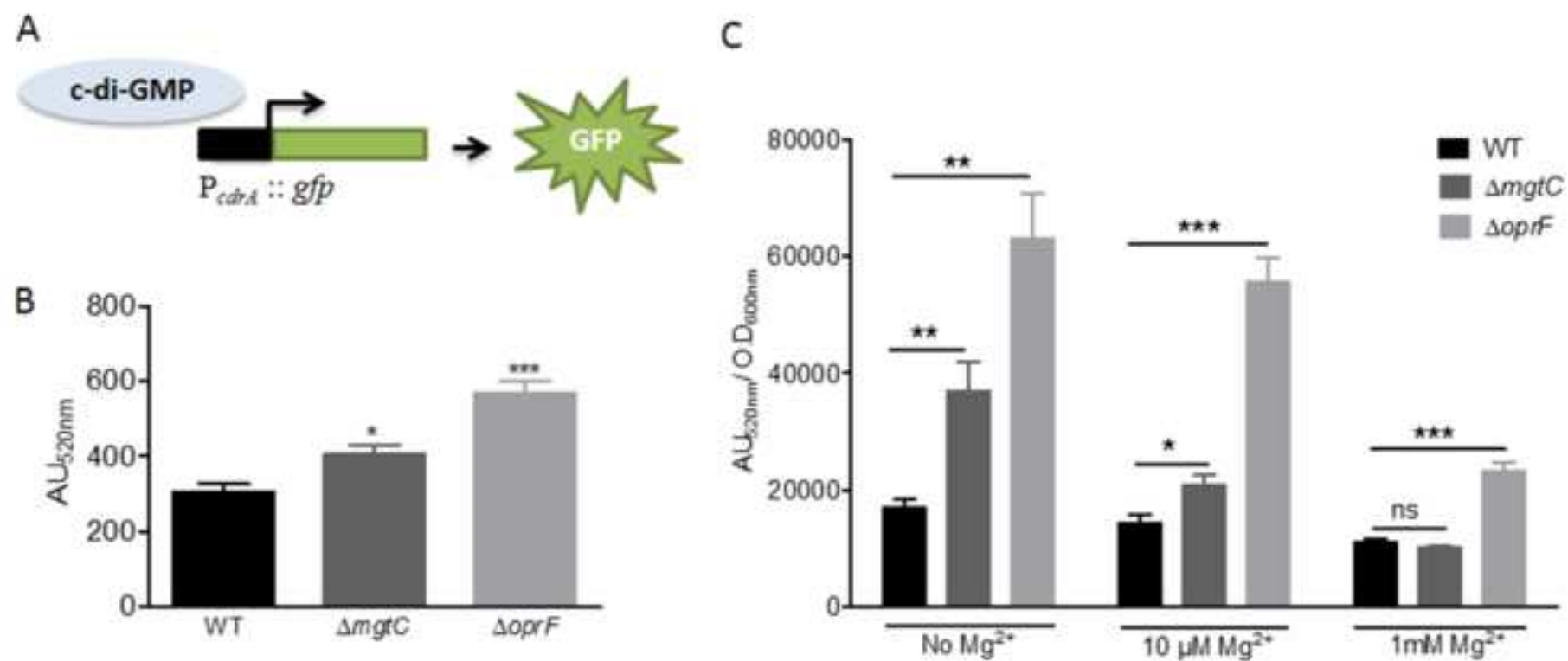
1036

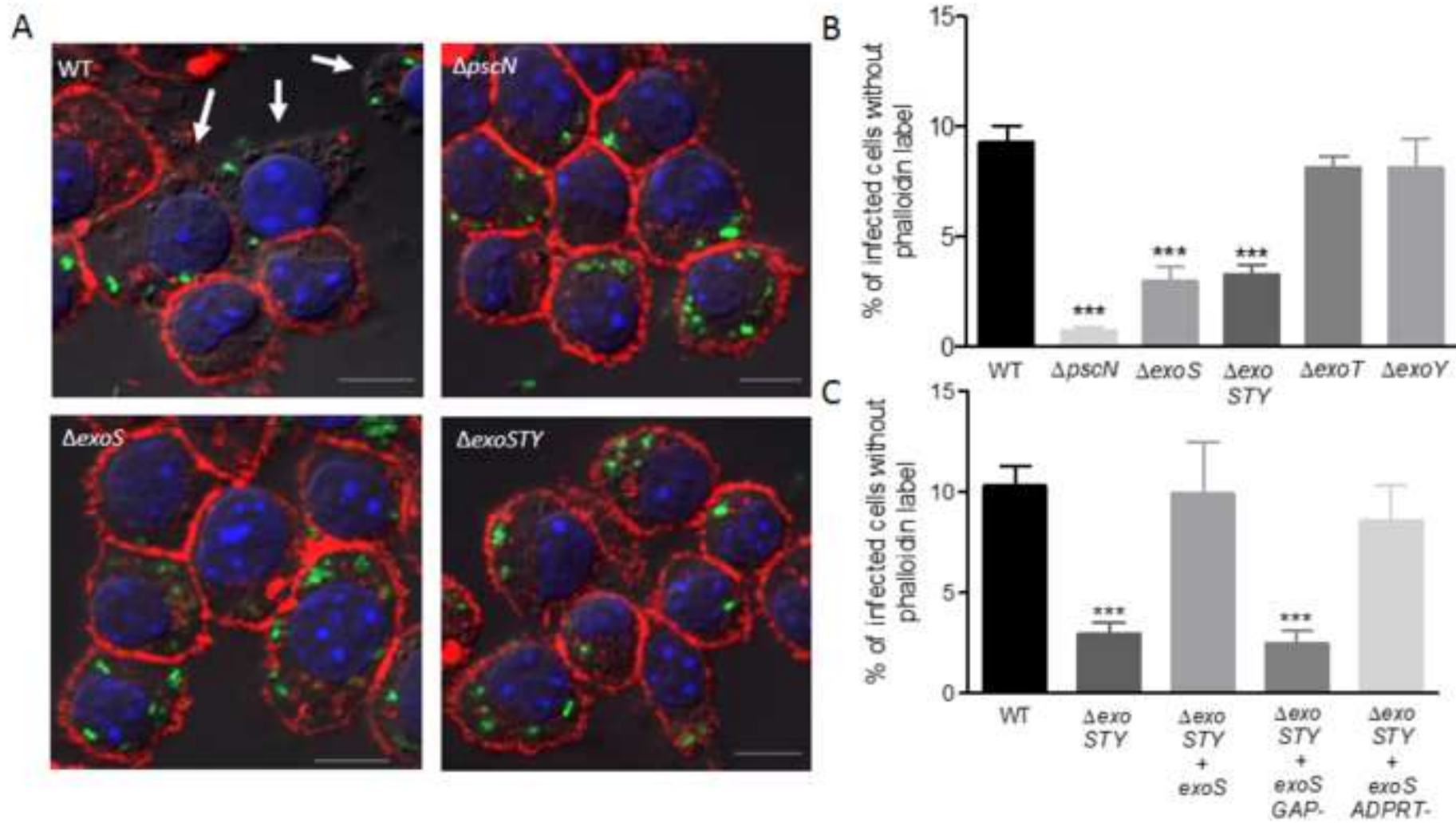


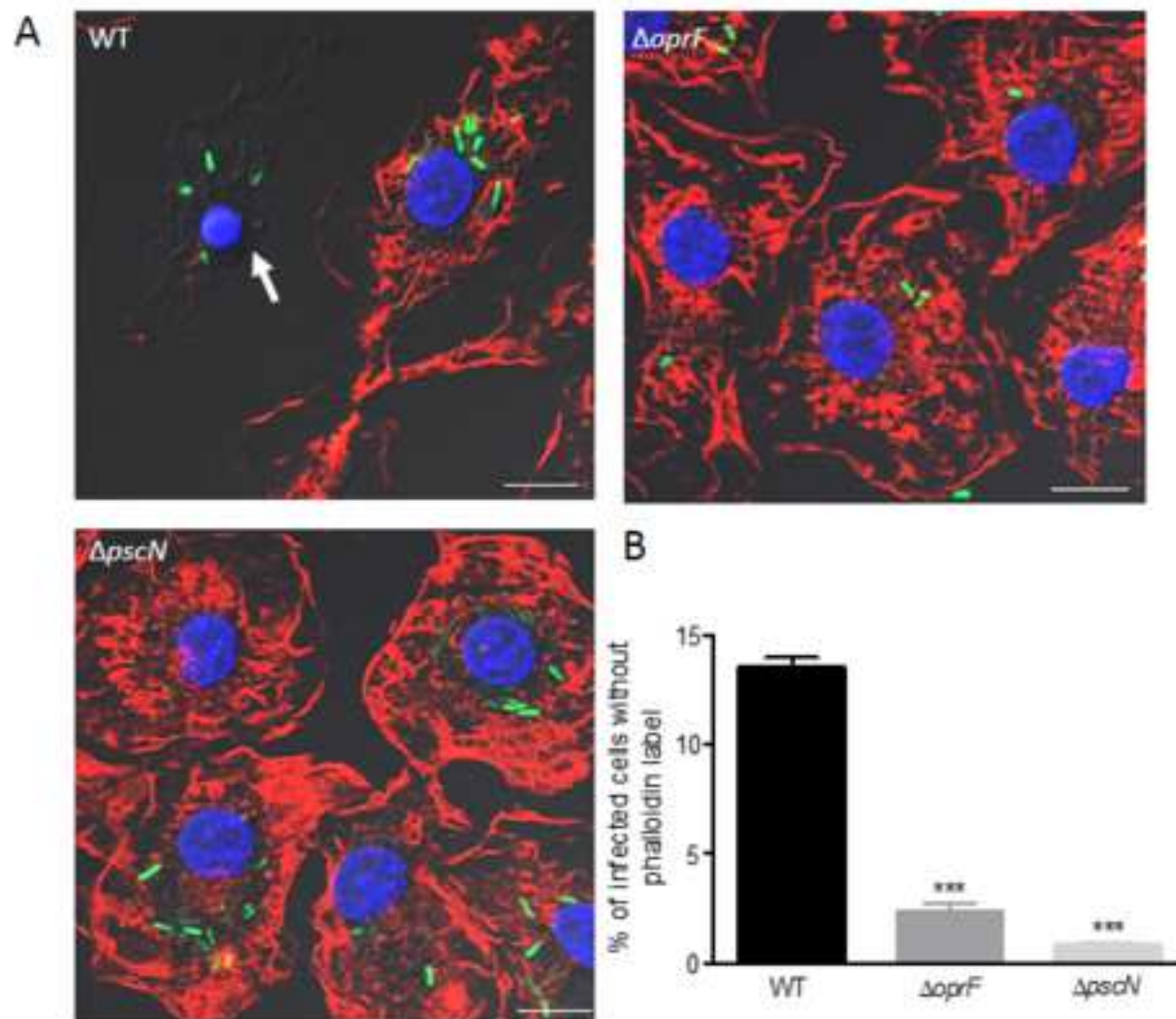


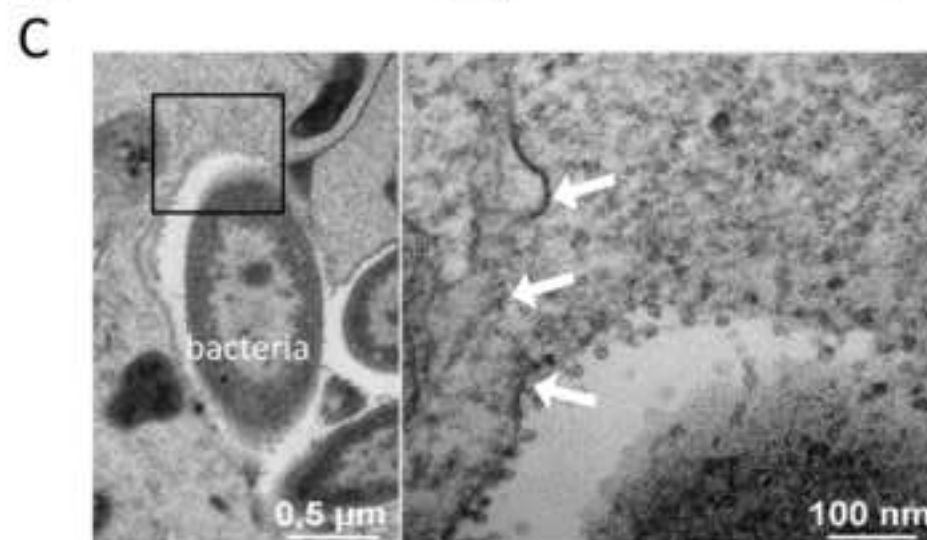
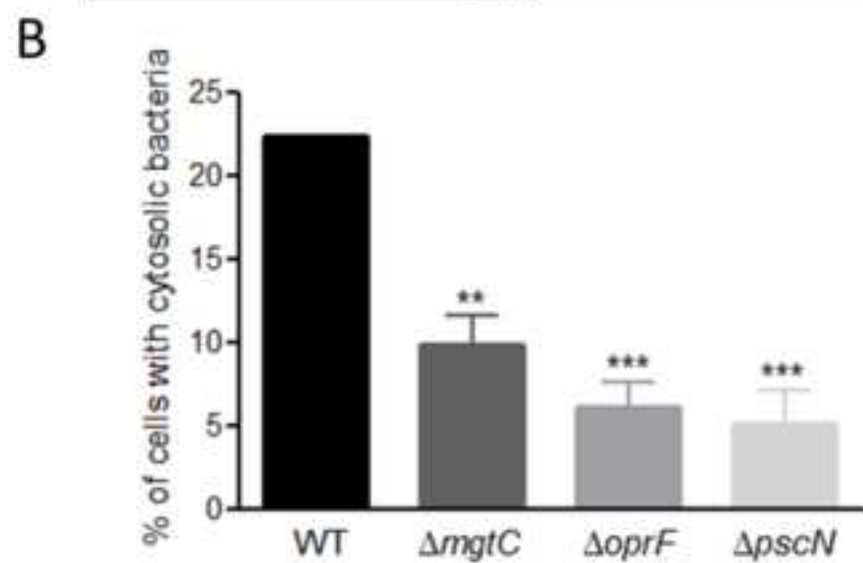
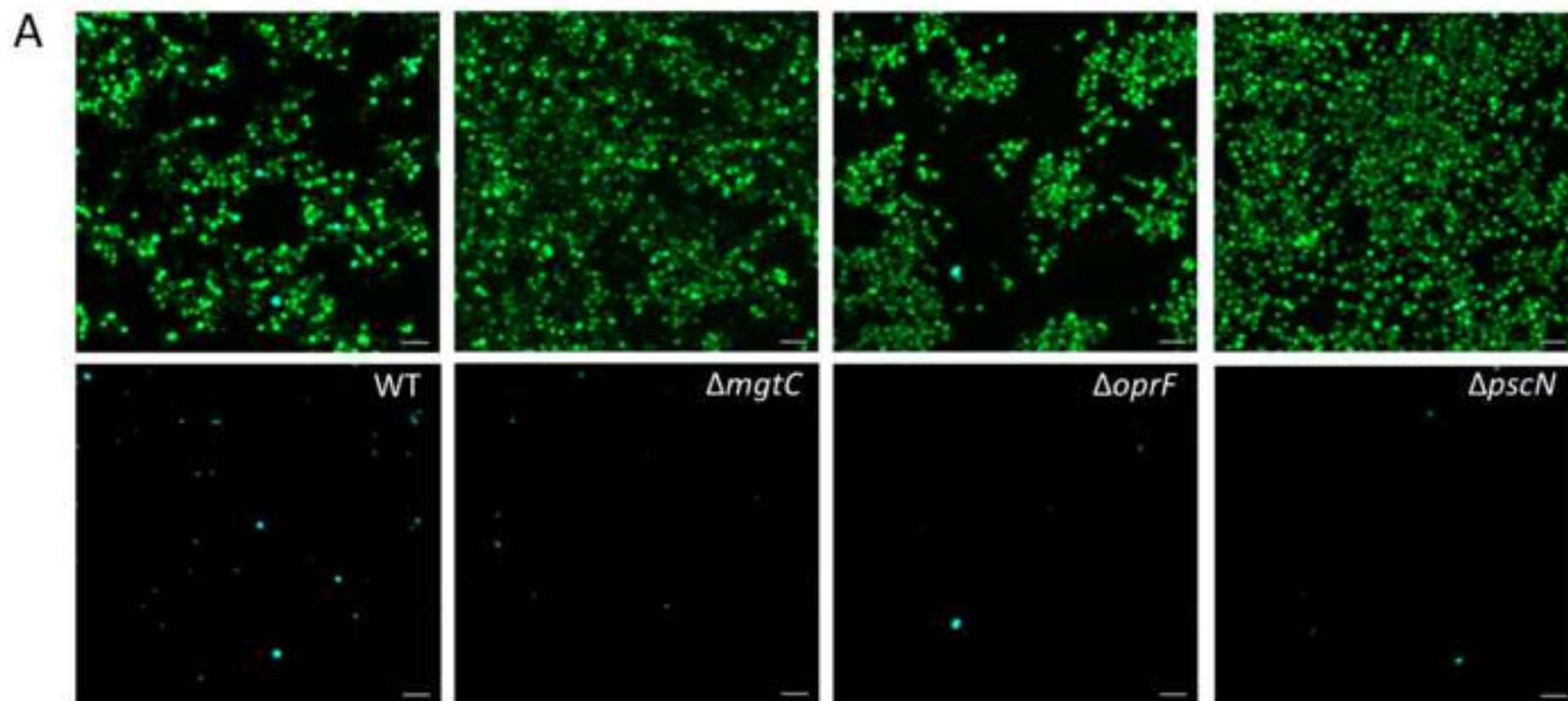


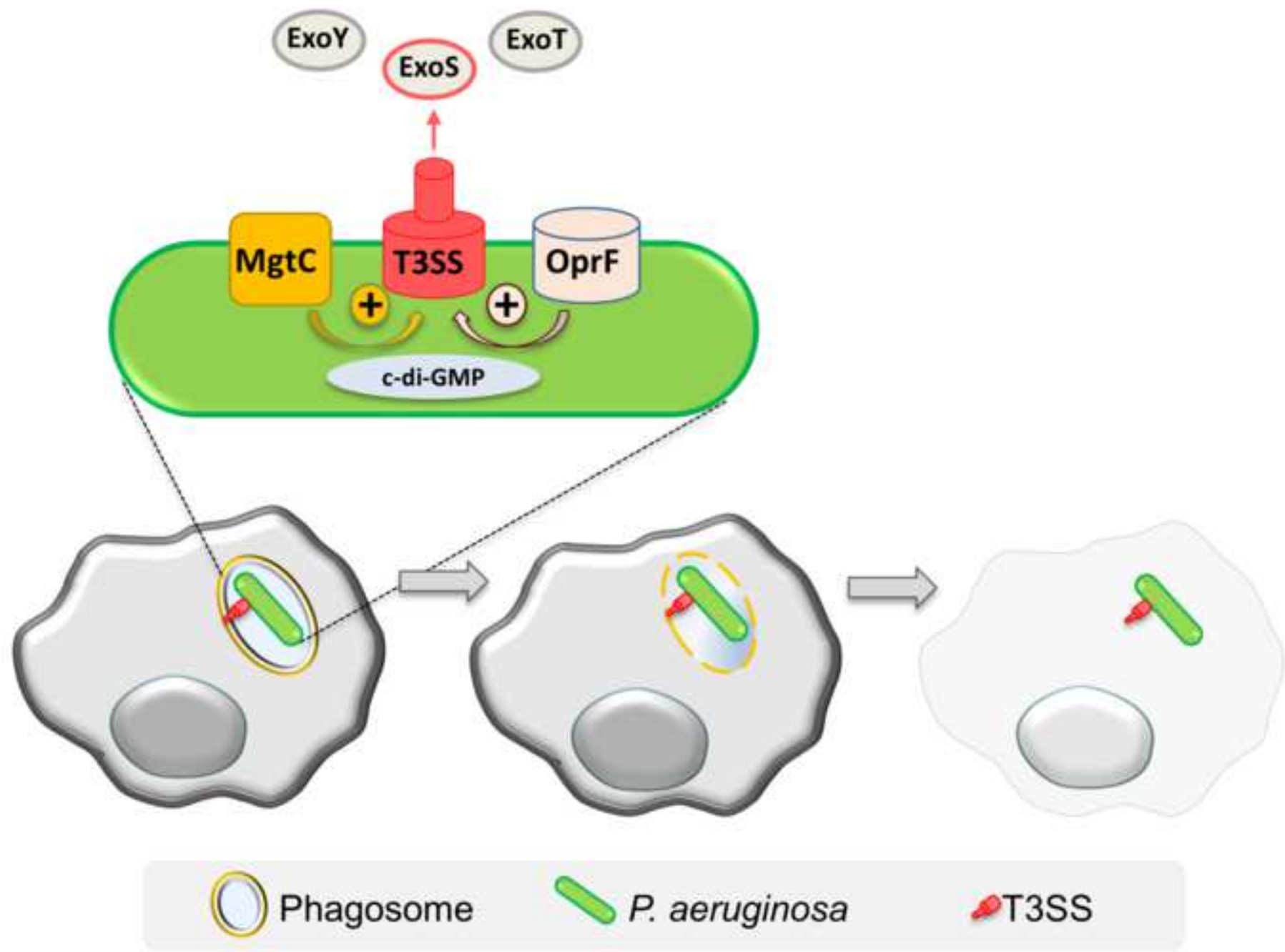














[Click here to access/download](#)

Supporting Information

Supplementary figures revised D-19-00097.pdf





Click here to access/download
Supporting Information
S1_Movie.mov



Click here to access/download
Supporting Information
S1_Table.pdf

1 **Killing from the inside: Intracellular role of T3SS in the fate of *Pseudomonas***
2 ***aeruginosa* within macrophages revealed by *mgtC* and *oprF* mutants**

3

4 Preeti Garai ¹, Laurence Berry ^{1#}, Malika Moussouni^{1#}, Sophie Bleves², Anne-Béatrice Blanc-
5 Potard^{1*}

6

7 ¹Laboratoire de Dynamique des Interactions Membranaires Normales et Pathologiques,
8 Université de Montpellier, CNRS-UMR5235, Montpellier, France

9 ²LISM, Institut de Microbiologie de la Méditerranée, CNRS & Aix-Marseille Univ, Marseille,
10 France.

11

12 [#]Both authors contributed equally to the work

13

14 *Corresponding author:

15 **E-mail: anne.blanc-potard@umontpellier.fr**

16

17 Running title: Intramacrophage fate of *Pseudomonas aeruginosa*

18 **Abstract**

19

20 While considered solely an extracellular pathogen, increasing evidence indicates that
21 *Pseudomonas aeruginosa* encounters intracellular environment in diverse mammalian cell
22 types, including macrophages. In the present study, we have deciphered the intramacrophage
23 fate of wild-type *P. aeruginosa* PAO1 strain by live and electron microscopy. *P. aeruginosa*
24 first resided in phagosomal vacuoles and subsequently could be detected in the cytoplasm,
25 indicating phagosomal escape of the pathogen, a finding also supported by vacuolar rupture
26 assay. The intracellular bacteria could eventually induce cell lysis, both in a macrophage cell
27 line and primary human macrophages. Two bacterial factors, MgtC and OprF, recently
28 identified to be important for survival of *P. aeruginosa* in macrophages, were found to be
29 involved in bacterial escape from the phagosome as well as in cell lysis caused by
30 intracellular bacteria. Strikingly, type III secretion system (T3SS) genes of *P. aeruginosa*
31 were down-regulated within macrophages in both *mgtC* and *oprF* mutants. Concordantly,
32 cyclic di-GMP (c-di-GMP) level was increased in both mutants, providing a clue for negative
33 regulation of T3SS inside macrophages. Consistent with the phenotypes and gene expression
34 pattern of *mgtC* and *oprF* mutants, a T3SS mutant ($\Delta pscN$) exhibited defect in phagosomal
35 escape and macrophage lysis driven by internalized bacteria. Importantly, these effects
36 appeared to be largely dependent on the ExoS effector, in contrast with the known T3SS-
37 dependent, but ExoS independent, cytotoxicity caused by extracellular *P. aeruginosa* towards
38 macrophages. Moreover, this macrophage damage caused by intracellular *P. aeruginosa* was
39 found to be dependent on GTPase Activating Protein (GAP) domain of ExoS. Hence, our
40 work highlights T3SS and ExoS, whose expression is modulated by MgtC and OprF, as key
41 players in the intramacrophage life of *P. aeruginosa* which allow internalized bacteria to lyse
42 macrophages.

43

44 **Author summary**

45

46 The ability of professional phagocytes to ingest and kill microorganisms is central to
47 host defense and *Pseudomonas aeruginosa* has developed mechanisms to avoid being killed
48 by phagocytes. While considered an extracellular pathogen, *P. aeruginosa* has been reported
49 to be engulfed by macrophages in animal models. Here, we visualized the fate of *P.*
50 *aeruginosa* within cultured macrophages revealing macrophage lysis driven by intracellular
51 *P. aeruginosa*. Two bacterial factors, MgtC and OprF, recently discovered to be involved in
52 the intramacrophage survival of *P. aeruginosa*, appeared to play a role in this cytotoxicity
53 caused by intracellular bacteria. We provided evidence that type III secretion system (T3SS)
54 gene expression is lowered intracellularly in *mgtC* and *oprF* mutants. We further showed that
55 intramacrophage *P. aeruginosa* uses its T3SS, specifically the ExoS effector, to promote
56 phagosomal escape and cell lysis. We thus describe a transient intramacrophage stage of *P.*
57 *aeruginosa* that could contribute to bacterial dissemination.

58

59

60

61 **Introduction**

62

63 Pathogenic bacteria are commonly classified as intracellular or extracellular pathogens
64 [1]. Intracellular bacterial pathogens, such as *Mycobacterium tuberculosis* or *Salmonella*
65 *enterica*, can replicate within host cells, including macrophages. In contrast, extracellular
66 pathogens, such as *Yersinia* spp., *Staphylococcus aureus*, *Pseudomonas aeruginosa* or
67 streptococci, avoid phagocytosis or exhibit cytotoxicity towards phagocytic cells, to promote
68 their extracellular multiplication. However, recent data have emphasized that several
69 extracellular pathogens can enter host cells *in vivo*, resulting in a phase of intracellular
70 residence, which can be of importance in addition to the typical extracellular infection. For
71 example, although *Yersinia* spp. subvert the functions of phagocytes from the outside, these
72 bacteria also subvert macrophage functions within the cell [2]. Once considered an
73 extracellular pathogen, it is now established that *S. aureus* can survive within many
74 mammalian cell types including macrophages [3,4] and the intramacrophage fate of *S. aureus*
75 has been deciphered [5,6]. Moreover, an intracellular phase within splenic macrophages has
76 been recently shown to play a crucial role in initiating dissemination of *Streptococcus*
77 *pneumoniae*, providing a divergence from the dogma which considered this bacterial
78 pathogen the classical example of extracellular pathogens [7].

79

80 The environmental bacterium and opportunistic human pathogen *P. aeruginosa* is
81 responsible for a variety of acute infections and is a major cause of mortality in chronically
82 infected cystic fibrosis (CF) patients. The chronic infection of *P. aeruginosa* and its resistance
83 to treatment is largely due to its ability to form biofilms, which relies on the production of
84 exopolysaccharides (EPS), whereas the type III secretion system (T3SS) is reported to play a

85 key role in the pathogenesis of acute *P. aeruginosa* infections [8]. Four T3SS effectors
86 (ExoU, ExoS, ExoT, ExoY) have been identified so far, ExoS being nearly always mutually
87 exclusive with the potent cytotoxin ExoU and more prevalent than ExoU [9-11]. ExoS has a
88 dual function as it contains a GTPase activating (GAP) domain as well as an ADP
89 ribosyltransferase (ADPRT) domain [10]. An intracellular step in airway epithelial cells has
90 been proposed to occur before the formation of biofilm during the acute phase of infection
91 [12,13] and the intracellular stage of *P. aeruginosa* within cultured epithelial cells has been
92 fairly studied [14-16]. The principle that *P. aeruginosa* is not exclusively an extracellular
93 pathogen has been convincingly established by the recent use of advanced imaging methods
94 to track bacteria within epithelial cells [17]. The T3SS, more specifically its effector ExoS,
95 has been implicated in the formation of membrane blebs-niche and avoidance of acidified
96 compartments to allow bacterial multiplication within epithelial cells [17-19]. Concordantly,
97 T3SS genes were recently shown to be expressed in *P. aeruginosa* internalized in epithelial
98 cells [17]. Regarding the interaction with macrophages, *P. aeruginosa* has developed
99 mechanisms to avoid phagocytosis [20]. However, *P. aeruginosa* has been shown to be
100 phagocytosed by macrophages in an acute model of infection in zebrafish embryos [21,22]
101 and has been reported to be engulfed by alveolar macrophages in the lungs of mice early after
102 pulmonary infection [23], suggesting that *P. aeruginosa* may need strategies to escape
103 macrophage killing. Although *P. aeruginosa* has been localized within cultured macrophages
104 during gentamicin protection assays [24-26], the intramacrophage fate of the bacteria has not
105 been characterized and bacterial factors involved in this step remain largely unexplored.

106

107 Bacterial survival in a particular niche requires the development of an adaptive
108 response, generally mediated by regulation of the bacterial genes involved in physiological
109 adaptation to the microenvironment. The identification of mutants lacking the ability to

110 survive within macrophages and the study of *P. aeruginosa* gene expression inside
111 macrophages is critical to determine bacterial players in this step. We have previously
112 uncovered MgtC as a bacterial factor involved in the intramacrophage survival of *P.*
113 *aeruginosa* [25,27]. In agreement with this intramacrophage role, expression of *Pseudomonas*
114 *mgtC* (PA4635) gene is induced when the bacteria reside inside macrophages [25]. MgtC is
115 known to promote intramacrophage growth in several classical intracellular bacteria,
116 including *Salmonella typhimurium* where it inhibits bacterial ATP synthase and represses
117 cellulose production [28-30], and is considered as a clue to reveal bacterial pathogens adapted
118 to an intramacrophage stage [30,31]. In addition, a recent study has implicated the outer
119 membrane protein OprF in the ability of otopathogenic *P. aeruginosa* strains to survive inside
120 macrophages [26]. OprF is an outer membrane porin that can modulate the production of
121 various virulence factors of *P. aeruginosa* [32,33].

122

123 In the present study, we investigated the fate of *P. aeruginosa* within macrophages
124 using wild-type PAO1 strain, which lacks ExoU, along with isogenic *mgtC* and *oprF* mutants.
125 We also explored, for the first time, the regulation of T3SS genes when *P. aeruginosa* resides
126 inside macrophages. The T3SS and ExoS effector, whose expression was found to be
127 modulated by MgtC and OprF intracellularly, were seemingly involved in this intracellular
128 stage, playing a role in vacuolar escape and cell lysis caused by intracellular bacteria.

129

130 **Results**

131

132 **Intracellular *P. aeruginosa* can promote macrophage lysis**

133 We previously visualized fluorescent *P. aeruginosa* residing within fixed macrophages [25].
134 To investigate the fate of *P. aeruginosa* after phagocytosis in a dynamic way, we monitored
135 macrophages infected with fluorescent bacteria using time-lapse live microscopy. J774
136 macrophages were infected with wild-type PAO1 strain expressing GFP grown exponentially
137 in LB medium (Multiplicity of infection or MOI=10). After 25 minutes of phagocytosis,
138 several washes were performed to remove adherent bacteria and gentamicin was added to kill
139 extracellular bacteria. Microscopic observation of infected macrophages up to 3 hours showed
140 cell lysis with increasing time (Fig 1), starting between 1.5 and 2 hours post-phagocytosis,
141 which can be attributed to intracellular bacteria as gentamicin was retained throughout the
142 experiment. No lysis of uninfected cells present in the same field was observed (Fig 1 and S1
143 Fig), as expected from an event due to intracellular bacteria rather than extracellular bacteria.
144 The cell lysis appeared to take place within a rapid time frame of few seconds, as shown by
145 the movie (S1 Movie), after which the bacteria seemed to be released from the host cell. We
146 also infected human monocyte-derived macrophages (HMDMs) with GFP producing PAO1
147 strain under similar conditions and found lysed infected cells after 2 hours of phagocytosis
148 (S2 Fig). Hence, the phenomenon of lysis of macrophages by intracellular PAO1 is not
149 restricted to J774 cell line, but is extendable to primary human macrophages.

150

151 We further examined intracellular *P. aeruginosa* within macrophages in more detail
152 using transmission electron microscopy (TEM). J774 macrophages infected with wild-type
153 PAO1 strain, were subjected to fixation at early time post-infection (30 min after
154 phagocytosis) or at later time of infection (3 hrs after phagocytosis). After phagocytosis, *P.*
155 *aeruginosa* was present in membrane bound vacuoles inside macrophages (Fig 2A). At a later
156 time point, some bacteria could be found in the cytoplasm with no surrounding membrane,
157 suggesting disruption of the vacuole membrane (Fig 2B). The infected macrophage was

158 damaged, displaying highly condensed chromatin and membrane blebbing, and lacking
159 pseudopodia. Healthy infected cells were also observed, where bacteria were mostly found in
160 vacuoles partially or totally filled with heterogeneous electron dense material, suggesting that
161 the vacuole has fused with lysosomes (Fig 2C). To confirm this, we examined the association
162 between fluorescent PAO1 bacteria and the LysoTracker probe during infection using fixed
163 macrophages. Bacteria colocalizing with LysoTracker could be visualized (S3 Fig), thereby
164 corroborating the TEM observation of fusion of vacuoles with lysosomes and the localization
165 of bacteria in acidified compartment.

166 TEM analyses allowed us to conclude that wild-type PAO1 strain has the ability to
167 reside within vacuoles and possibly escape from the phagosome into the cytoplasm and
168 promote cell damage. A rapid cell lysis event caused by intracellular *P. aeruginosa* visualized
169 by live microscopy revealed that phagocytosed bacteria can escape from macrophage through
170 cell lysis.

171

172 **Intracellular *mgtC* and *oprF* mutants are compromised in cell lysis**

173 Our previous results based on gentamicin protection assay on J774 infected macrophages and
174 counting of colony forming units (CFU) indicated that *mgtC* mutant (generated in the PAO1)
175 background) survived to a lesser extent than the wild-type strain [25]. More recently, an *oprF*
176 mutant of an otopathogenic strain of *P. aeruginosa* was also found to be defective in
177 intracellular survival in mouse bone marrow macrophages based on gentamicin protection
178 assay [26]. To analyze the phenotypes of *oprF* mutant in the PAO1 background towards J774
179 macrophages and compare that with *mgtC* mutant, we used here a previously described *oprF*
180 mutant generated in PAO1 strain [25,34].

181 Based on the finding that intracellular *P. aeruginosa* can cause macrophage lysis, we
182 developed a suitable assay using fluorescent microscopic analysis to quantify cell damage
183 caused by intracellular bacteria. Macrophages were infected with fluorescent bacteria, treated
184 with gentamicin for 2 hours after phagocytosis, fixed and stained with phalloidin-TRITC to
185 label F-actin and visualize macrophage morphology. A clear cortical red labeling was seen in
186 most cells, which is indicative of the plasma membrane-associated cortical actin. Few infected
187 cells appeared lysed due to the loss of cortical actin staining (Fig 3A), which agrees with the
188 observation of lysed macrophages in time lapse fluorescence microscopy (Fig 1). The loss of
189 cortical actin staining was found to be due to internalized bacteria because upon arresting
190 phagocytosis, by treating macrophages with cytochalasin D, bacteria were not internalized
191 and loss of cortical actin staining was not observed (S4 Fig). Hence, any delayed effect of
192 extracellular bacteria occurring before gentamicin treatment or a contribution of extracellular
193 bacteria that would resist gentamicin treatment can be ruled out. Quantification of the number
194 of cells without phalloidin labelling showed highest value for wild-type strain, intermediate
195 for *mgtC* mutant and lowest for *oprF* mutant (Fig 3B). Thus, both intracellular *mgtC* and *oprF*
196 mutants appeared compromised for cell lysis. This feature is not linked to a lower
197 internalization rate of the mutant strains, because *mgtC* mutant is known to be more
198 phagocytosed than wild-type strain [25] and a similar trend was found for *oprF* mutant (not
199 shown). Since T3SS has been involved in the intracellular life of *P. aeruginosa* in other cell
200 types [17], we next monitored the expression of T3SS genes during the residence of bacteria
201 within macrophages.

202

203 **Down-regulation of T3SS gene expression in *mgtC* and *oprF* mutants inside**
204 **macrophages**

205 The *P. aeruginosa oprF* mutant was reported to be defective in the secretion of T3SS
206 effectors in liquid culture and in the production of PcrV, the T3SS needle tip protein [32,34],
207 but the effect of OprF on transcription of T3SS genes has not been tested so far. We thus
208 investigated the expression of the effector gene *exoS* along with the gene *pcrV* in *oprF* mutant
209 strain in comparison to wild-type strain upon macrophage infection. As a control, we tested
210 flagellin coding gene *fliC*, which is not part of the T3SS regulon, but was proposed to be
211 secreted by the T3SS [35]. Expression of both *pcrV* and *exoS* genes was found to be highly
212 reduced in the *oprF* mutant (Fig 4). Strikingly, the *mgtC* mutant also exhibited significantly
213 reduced expression of these two T3SS genes (Fig 4), although to a lesser extent than the *oprF*
214 mutant, indicating an unexpected interplay between MgtC and T3SS. On the other hand, *fliC*
215 expression was not altered in both mutants.

216 Since we observed a decreased transcriptional level of T3SS genes in the *oprF* mutant,
217 we further examined the link between intramacrophage expression of T3SS and cell lysis in
218 this mutant. A recombinant plasmid allowing IPTG-inducible overproduction of ExsA, a
219 master transcriptional activator of T3SS genes [36], was introduced in the *oprF* mutant. Upon
220 induction of *exsA* expression with 0.01 mM IPTG, *oprF* mutant promoted macrophage lysis
221 like the wild-type strain (S5 Fig), supporting a model whereby the effect of OprF is the result
222 of its positive regulatory effect on T3SS expression.

223 To address the mechanism behind the downregulation of transcription of T3SS in *oprF*
224 and *mgtC* mutant strains, we evaluated the level of the second messenger c-di-GMP, as it is
225 known to participate in T3SS repression in *P. aeruginosa* [37]. The *oprF* mutant was already
226 reported to have high production of c-di-GMP in liquid culture [34]. We used a fluorescence-
227 based reporter (Fig 5A) that has been validated to gauge c-di-GMP level inside *P. aeruginosa*
228 [38]. The pCdrA::*gfp* plasmid was introduced into wild-type and mutant strains, and
229 fluorescence was measured in infected macrophages (Fig 5B). Both *oprF* and *mgtC* mutants

230 exhibited significantly increased activity of the *cdrA* promoter comparatively to wild-type
231 strain, indicative of higher levels of c-di-GMP than the wild-type strain. To better appreciate
232 the differences monitored within macrophages, we also measured fluorescence of strains
233 grown in culture medium with various magnesium concentrations (Fig 5C). The *oprF* mutant
234 exhibited a two to three-fold increase in the activity of the *cdrA* promoter comparatively to
235 wild-type strain, which is in the same range as the increase observed within macrophages (Fig
236 5B), and agrees with published data obtained with this indirect strategy and direct c-di-GMP
237 measurement [34]. Under magnesium limitation, a condition known to induce the expression
238 of *mgtC*, the *mgtC* mutant also showed increased activity of the *cdrA* promoter comparatively
239 to wild-type strain, with a two-fold increase in the absence of Mg^{2+} , and a minor, but
240 significant, increase in the presence of 10 μM Mg^{2+} that is similar to what is observed within
241 macrophages. On the other hand, the level of fluorescence of wild-type strain and *mgtC*
242 mutant was identical in medium supplemented with 1 mM Mg^{2+} , a condition that prevents
243 *mgtC* expression [25]. Taken together, these results indicate that the production of c-di-GMP
244 is increased relatively to wild-type strain in both *oprF* and *mgtC* mutants, with a more
245 pronounced effect for *oprF*, when bacteria reside within macrophages, thus providing a
246 mechanistic clue for the negative effect on T3SS gene expression.

247

248 **A T3SS mutant is defective for cell death driven intracellularly in an ExoS-dependent** 249 **manner**

250 Given the effect of both *oprF* and *mgtC* deletions on the expression of T3SS genes within
251 macrophages, we investigated the fate of a T3SS mutant upon phagocytosis. We first used a
252 *pscN* mutant that is defective for the ATPase function of the T3SS machinery [36].
253 Intracellular T3SS mutant did not induce loss of cortical phalloidin staining, as shown by
254 fluorescent imaging and subsequent quantification, indicating lack of cell lysis (Fig 6A and

255 B). Thus, the phenotype of T3SS mutant is consistent with that of *mgtC* and *oprF* mutants and
256 in correlation with their level of T3SS gene expression. We further examined the relevance of
257 our findings to primary human macrophages, by assessing the lysis of HMDMs driven
258 intracellularly by wild-type *P. aeruginosa* or *oprF* and *pscN* mutants. The count of
259 intracellularly lysed cells was significantly different between wild-type and each mutant strain
260 (Fig 7), with a similar trend to that of J774 macrophages (Fig 3 and Fig 6), thus confirming
261 the importance of T3SS in intracellularly driven lysis of primary macrophages as well.

262

263 To address the implication of T3SS effector proteins in this process, we used
264 individual effector mutant strains *exoS*, *exoT*, *exoY* and the triple mutant *exoSTY*. The
265 intracellular lysis of macrophages was found to be reduced for the triple mutant *exoSTY* and
266 to a similar extent for the *exoS* mutant (Fig 6A and B), suggesting a major contribution of
267 ExoS. Accordingly, *exoT* and *exoY* mutants behave similarly to wild-type strain (Fig 6B).
268 Moreover, complementation of the *exoSTY* mutant with *exoS* restored the wild-type
269 phenotype (Fig. 6C). Although the lysis by *exoS* mutant strain was substantially higher than
270 that of *pscN* mutant, these results suggest that the T3SS-mediated intracellular lysis of
271 macrophages by *P. aeruginosa* relies mainly on the T3SS effector ExoS. Thus, this ExoS-
272 dependent cytotoxic effect mediated by intracellular bacteria differs from the classical T3SS-
273 dependent cytotoxicity driven by extracellular bacteria towards macrophages that has been
274 reported to be mostly independent of ExoS [39-41]. To confirm this difference between
275 intracellular and extracellular bacteria mediated lysis, we measured the lactate dehydrogenase
276 (LDH) release when infection was carried out without removing extracellular bacteria. As
277 expected, similar values were obtained for wild-type strain and *exoS* mutant, whereas a *pscN*
278 mutant showed significantly reduced LDH release (S6 Fig), which agrees with the reported
279 T3SS-dependent but ExoS independent cytotoxicity caused by extracellular bacteria. This is

280 consistent with trypan blue exclusion assay, which monitors cell death based on penetration of
281 a membrane impermeable dye, when the assay is done immediately after phagocytosis (S7
282 Fig, panel A).

283 ExoS possesses both GAP domain as well as ADPRT domain and complementing
284 strains retaining only one of these two domains have been constructed earlier [42]. To address
285 which domain of ExoS plays role in intracellular cytotoxicity, we carried out the phalloidin-
286 based lysis assay using the *exoSTY* mutant producing either ADPRT (GAP-) or GAP
287 (ADPRT-) domain of ExoS. Our results clearly showed that the strain retaining GAP activity
288 of ExoS but lacking ADPRT activity (Δ *exoSTY* + *exoS* ADPRT-) could complement the
289 phenotype to an extent similar to the strain complemented with *exoS* (Fig. 6C), which is also
290 equivalent to the wild-type. To strengthen our findings, we performed trypan blue exclusion
291 assay after 2hrs of gentamicin treatment. The results are consistent with phalloidin assay,
292 supporting the implication of ExoS, and more specifically its GAP domain, for macrophage
293 death induced by intracellular bacteria (S7 Fig, panel B). This contrasts with the results of
294 trypan blue exclusion assay performed immediately after phagocytosis, where a low level of
295 T3SS-dependent cell death is observed, but not linked to ExoS function (S7 Fig, panel A).

296 Hence, our results indicate that, in contrast to extracellular *P. aeruginosa*, intracellular
297 *P. aeruginosa* uses an ExoS-dependent T3SS mediated mechanism to promote macrophage
298 lysis. Moreover, only the GAP activity of ExoS is required for this process.

299

300 ***P. aeruginosa* T3SS, *oprF* and *mgtC* mutants displayed lower vacuolar escape than wild-
301 type PAO1**

302 The phagosomal environment of the macrophage is hostile for bacterial pathogens and TEM
303 analysis indicated that PAO1 can be found in the cytoplasm, suggesting escape from the

304 phagosomal vacuole (Fig 2B). We decided to address the intracellular role of T3SS, OprF and
305 MgtC in the phagosomal escape of *P. aeruginosa* to the cytoplasm of macrophages. To
306 monitor *P. aeruginosa* escape from phagosome, we used the CCF4-AM/ β -lactamase assay
307 that has been developed for tracking vacuolar rupture by intracellular pathogens [43]. This
308 assay takes advantage of the natural production of β -lactamase by *P. aeruginosa* [44], which
309 can cleave a fluorescent β -lactamase substrate, CCF4-AM, that is trapped within the host
310 cytoplasm. CCF4-AM emits a green fluorescence signal, whereas in the presence of β -
311 lactamase activity, a blue fluorescence signal is produced. The detection of blue fluorescent
312 cells at 2 hrs post-phagocytosis indicated bacterial escape from the phagosome to the
313 cytoplasm (Fig 8A). The escape of wild-type strain was compared to that of *mgtC*, *oprF* and
314 *pscN* mutants by quantifying the percentage of blue fluorescent cells out of total green
315 fluorescent cells. Wild-type strain showed significantly higher percentage of phagosomal
316 escape than all mutants tested (Fig 8B). No significant difference in terms of cleavage of
317 CCF4-AM was measured for the mutants with respect to wild-type in liquid cultures (S8 Fig),
318 indicating that the lower amount of blue fluorescent cells with the mutants is not due to
319 reduced production of endogenous β -lactamase. In agreement with the finding of phagosomal
320 escape by CCF4-AM/ β -lactamase assay, ruptured phagosomal membrane could be visualized
321 by TEM in macrophages infected with PAO1 wild-type strain (Fig 8C). Both *exoS* and
322 *exoSTY* effector mutants also displayed a low percentage of phagosomal escape, which
323 appeared similar to that of *pscN* mutant (S9 Fig). These results indicate that the T3SS,
324 through the ExoS effector, plays role in the escape of *P. aeruginosa* from the phagosome to
325 the cytoplasm. The effect of MgtC and OprF in this process may as well be mediated by their
326 effect on T3SS gene expression (Fig 4).

327 Cumulatively, our results support a T3SS-dependent vacuolar escape for *P.*
328 *aeruginosa*, leading to the localization of bacteria in the cytoplasm and cell lysis as depicted
329 in the proposed model (Fig 9).

330

331 **Discussion**

332

333 The ability of professional phagocytes to ingest and kill microorganisms is central to
334 innate immunity and host defense. *P. aeruginosa* is known to avoid being killed by
335 phagocytes through the destruction of immune cells extracellularly as well as avoidance of
336 phagocytosis [20]. However, *P. aeruginosa* has been reported to be engulfed by macrophages
337 in animal infection models [21-23]. In addition, *P. aeruginosa* has been visualized in
338 phagocytes in cell culture models in several studies, where MgtC and OprF have been shown
339 to be involved in the ability of *P. aeruginosa* to survive in cultured macrophages [25,26]. The
340 virulence of *P. aeruginosa mgtC* mutant can be restored in zebrafish embryos upon
341 macrophages depletion, suggesting that MgtC acts to evade phagocytes [25]. Interestingly, a
342 similar behavior has been reported for a T3SS mutant in the same infection model [21]. We
343 show here that MgtC and OprF regulate T3SS when *P. aeruginosa* resides in macrophages
344 and we describe a novel strategy used by *P. aeruginosa* to escape from macrophages that
345 relies on a T3SS-dependent cell lysis induced by intracellular bacteria (Fig. 9).

346

347 Using electron microscopy, we demonstrate that upon phagocytosis, *P. aeruginosa*
348 PAO1 strain resides in membrane bound vacuoles, whereas a cytosolic location can be
349 observed at later time of infection, which corroborates the observation of an otopathogenic *P.*
350 *aeruginosa* clinical strain in HMDMs [26]. Microscopic analysis of live and fixed cells

351 revealed macrophage lysis driven by intracellular bacteria, both with J774 macrophage cell
352 line as well as HMDMs. This cell lysis is a rapid process associated with the loss of cortical
353 actin from plasma membrane. We propose that the cell lysis induced by intracellular *P.*
354 *aeruginosa* is linked to the phagosomal escape of bacteria as indicated by the observation of
355 cytosolic bacteria and ruptured phagosomal membrane by TEM as well as CCF4-AM/ β -
356 lactamase based phagosomal rupture assay.

357

358 To better characterize the *P. aeruginosa* factors involved in its intramacrophage fate,
359 we investigated intracellular expression of T3SS genes in *mgtC* and *oprF* mutants. Expression
360 of T3SS genes upon macrophage infection was significantly decreased in *mgtC* mutant and
361 abrogated in *oprF* mutant. The production of T3SS effectors or needle component was
362 previously known to be altered in the *oprF* mutant [32,34], but a direct effect at the
363 transcriptional level was not investigated before. This regulation could be mediated by c-di-
364 GMP, a known negative regulator of T3SS expression [37], as the reporter assay revealed an
365 increased level of c-di-GMP in both *oprF* and *mgtC* mutants upon monitoring infected
366 macrophages, with a more pronounced effect for *oprF* mutant. An increased level of c-di-
367 GMP in *oprF* mutant is consistent with previous results obtained *in vitro* [34]. The moderate,
368 but significant, increased level of c-di-GMP in *mgtC* mutant in macrophages with respect to
369 wild-type strain is equivalent to the fold increase obtained in low-Mg²⁺ cultures. It is of
370 interest to note that a *Salmonella mgtC* mutant also exhibited increased c-di-GMP level
371 intracellularly and under low-Mg²⁺ condition [29]. The *P. aeruginosa mgtC* and *oprF* mutants
372 showed a moderate and a more pronounced decrease, respectively, in cytotoxicity driven by
373 intracellular bacteria and phagosomal escape. These phenotypes could be linked to the pattern
374 of T3SS expression in *mgtC* and *oprF* mutants, because a T3SS mutant appeared to lack
375 cytotoxicity driven by intracellular bacteria and showed reduced phagosomal escape.

376 Accordingly, inducing expression of *exsA* gene, a master activator of T3SS, in *oprF* mutant
377 promoted macrophage lysis driven by intracellular bacteria to a similar level to that of wild-
378 type strain, supporting the model whereby the phenotype of *oprF* mutant is the result of a
379 negative regulation of T3SS expression.

380

381 Our data indicate that the T3SS-mediated cytotoxicity driven by intracellular *P.*
382 *aeruginosa* is largely dependent on the ExoS effector. ExoS, which has a dual function [10],
383 is known to play a role in *P. aeruginosa* intracellular life in cell types other than
384 macrophages. The T3SS and ExoS are indeed key factors for intracellular replication of *P.*
385 *aeruginosa* in epithelial cells, with a main role of the ADPRT domain in the formation of
386 replicative niche in membrane blebs [18,19,45]. ExoS and ExoT ADPRT domains also
387 promote bacterial survival in neutrophils [46], by having a protective role against NADPH-
388 oxidase activity [47]. However, the effect of T3SS towards macrophages was so far restricted
389 to the well-known cytotoxicity caused by extracellular *P. aeruginosa* [39,48-50]. In *P.*
390 *aeruginosa* strains lacking ExoU toxin, such as PAO1, this cytotoxicity is due to
391 inflammasome activation, which is dependent on T3SS translocation apparatus, but is
392 independent of the ExoS effector [39-41,51]. Accordingly, this T3SS-dependent ExoS-
393 independent cytotoxicity was observed in our assays when extracellular bacteria are not
394 removed. In contrast, upon removal of extracellular bacteria, a T3SS-mediated cytotoxicity
395 implicating ExoS was uncovered. Hence, ExoS appears to be associated with cell damage
396 only when it is secreted from internalized bacteria. Moreover, phagosomal rupture assay
397 indicated that ExoS plays role in the escape of *P. aeruginosa* from the phagosome to the
398 cytoplasm and we propose that upon phagosomal rupture, the cytoplasmic location of *P.*
399 *aeruginosa* induces inflammasome, possibly through the release of bacterial
400 lipopolysaccharides (LPS) in the cytoplasm, which would promote cell death. Therefore, in

401 addition to the inflammasome activation caused by extracellular *P. aeruginosa* and, as very
402 recently described, by intracellular T3SS-negative *P. aeruginosa* in the context of long-term
403 infection [52], our study suggests that inflammasome and subsequent macrophage death can
404 also be caused by intracellular T3SS-positive *P. aeruginosa*. Further experiments will be
405 required to characterize inflammasome activation and pathways that lead to cell death.

406

407 The intracellular implication of ExoS in both macrophages and epithelial cells
408 suggests that the intracellular life of *P. aeruginosa* in macrophages shares features with the
409 intracellular life of the pathogen in epithelial cells, even though the outcome is different.
410 Whereas bacteria actively replicate in epithelial cells, within bleb niches or in the cytosol
411 [17], replication of bacteria is barely seen within macrophages resulting instead in cell lysis
412 and bacterial escape from macrophages. Our results further indicate that the macrophage
413 damage caused by intracellular bacteria is due to ExoS GAP domain, which thus differs from
414 the reported role of the ADPRT domain of ExoS in blebs formation associated with *P.*
415 *aeruginosa* intracellular replication within epithelial cells [18,19,45]. On the other hand, the
416 implication of GAP domain of ExoS towards epithelial cells in promoting cell rounding, actin
417 reorganization or cell death has not been specifically associated with intracellular bacteria
418 [53,54]. Although ExoS and ExoT GAP domain have similar biochemical activities, these
419 effectors may differ in their localization inside host cells or they may interact with different
420 host factors to bring about their effect. This is supported by the fact that induction of
421 apoptosis in epithelial cells by ExoT GAP domain, a feature that was not reported for ExoS
422 GAP domain [55] and by our finding that, unlike ExoS, ExoT is not involved in the
423 intramacrophage phenotypes. Importantly, we showed that the extent of phagosomal escape
424 of *pscN* and *exoSTY* mutants was similar to that of *exoS* mutant alone, suggesting that ExoS is
425 the main effector protein involved in the exit of *P. aeruginosa* from the phagosome. In

426 epithelial cells, ExoS has been involved in avoidance of acidified compartment [18,19].
427 Considering our findings, ExoS may allow avoidance of acidification in macrophages and
428 may also contribute to the vacuolar escape in epithelial cells. Further studies will be required
429 to decipher in more detail, the function of ExoS inside macrophages, including a better
430 understanding of its role in phagosomal escape and identification of its host targets within
431 macrophages. ExoS-positive strains represent a large amount of clinical isolates but the
432 number of ExoS-negative strains is nevertheless substantial (about one third of isolates),
433 especially among strains associated with bacteremia [10,11,56]. However, strains lacking
434 ExoS usually encode the potent cytotoxin ExoU, thus exhibiting high toxicity towards
435 eukaryotic cells from outside and less susceptibility to encounter an intracellular stage.

436

437 In conclusion, our results indicate that *P. aeruginosa* shares common feature with
438 other so-called extracellular pathogens, such as *S. aureus*, which can reside transiently within
439 macrophages [4] and require bacterial factors to survive this stage [57]. The present study
440 uncovered bacterial factors allowing internalized *P. aeruginosa* to lyse macrophages. This
441 should allow bacteria to evade macrophages and an important issue now is to better evaluate
442 the contribution of intramacrophage stage to disease outcome during *P. aeruginosa* infection.
443 Survival of *P. aeruginosa* within macrophages and subsequent bacterial release may play a
444 role in the establishment and dissemination of infection. There is also evidence that
445 intracellular survival may contribute to persistence of the infection by creating a niche
446 refractory to antibiotic action [24], highlighting the potential importance of this overlooked
447 phase of *P. aeruginosa* infection.

448

449 **Materials and methods**

450

451 **Bacterial strains and growth conditions**

452 Bacterial strains and plasmids are described in Table 1. *P. aeruginosa* mutant strains (all in
453 the PAO1 background) have been described and phenotypically characterized previously
454 (Table 1). The *oprF* mutant (strain H636) is derived from PAO1 wild-type strain H103 [34],
455 which exhibits the same level of ExoS secretion under T3SS-inducing conditions as PAO1,
456 isogenic strain for *mgtC* and T3SS mutants (S10 Fig). *P. aeruginosa* was grown at 37°C in
457 Luria broth (LB). Growth in magnesium-defined medium was done in NCE-minimal medium
458 [58] supplemented with 0.1% casamino acids, 38 mM glycerol, without MgSO₄ or containing
459 10 μM or 1mM MgSO₄. Plasmid pMF230 expressing GFP constitutively [59] (obtained from
460 Addgene), was introduced in *P. aeruginosa* by conjugation, using an *E. coli* strain containing
461 helper plasmid pRK2013. Recombinant bacteria were selected on *Pseudomonas* isolation agar
462 (PIA) containing carbenicillin at the concentration of 300 μg/ml.

463

464 **Table 1. Bacterial strains and plasmids used in the study**

Name	Description	Reference
PAO1		Laboratory collection
PAO1 $\Delta mgtC$	$\Delta mgtC$	[25]
H636	$\Delta oprF$	[34]
PAO1 $\Delta pscN$	$\Delta pscN$ T3SS ATPase mutant	[36]
PAO1 $\Delta exoS$	$\Delta exoS$	[50]

PAO1 Δ <i>exoY</i>	Δ <i>exoY</i>	[50]
PAO1 Δ <i>exoT</i>	Δ <i>exoT</i>	[50]
PAO1 Δ <i>exoSTY</i>	Δ <i>exoSTY</i>	[50]
PAO1F Δ 3Tox/ExoS	Δ <i>exoS</i> Δ <i>exoT</i> Δ <i>exoY</i> <i>attB::exoS</i>	[42]
PAO1F Δ 3Tox/ExoS _{GAP-}	Δ <i>exoS</i> Δ <i>exoT</i> Δ <i>exoY</i> <i>attB::exoS-R_{146K}</i>	[42]
PAO1F Δ 3Tox/ExoS _{ADPR -}	Δ <i>exoS</i> Δ <i>exoT</i> Δ <i>exoY</i> <i>attB::exoS-E_{379D/E_{381D}}</i>	[42]
pRK2013	Tra ⁺ , Mob ⁺ , ColE1, Km ^r	Laboratory collection
pMF230	GFP _{mut2} , Amp ^r	[59]
pTn7CdrA:: <i>gfp^C</i>	Amp ^r , Gm ^r	[38]
pSBC6	<i>exsA</i> cloned in pMMB190 under control of <i>tacp</i> Amp ^r	[36]

465

466

467 **Infection of J774 macrophages**

468 J774 cells (mouse macrophage cell line J774A.1, gifted by Gisèle Bourg, Inserm U 1047,
469 Nîmes, France) were maintained at 37°C in 5% CO₂ in Dulbecco's modified Eagle medium
470 (DMEM) (Gibco) supplemented with 10% fetal bovine serum (FBS) (Gibco). The infection of
471 J774 macrophages by *P. aeruginosa* was carried out essentially as described previously [25].

472 Mid-log phase *P. aeruginosa* grown in LB broth was centrifuged and resuspended in PBS to
473 infect J774 macrophages (5×10^5 cells/well) at an MOI of 10. After centrifugation of the 24-
474 well culture plate for 5 min for synchronization of infection, bacterial phagocytosis was
475 allowed for 25 min. Cells were washed three times with sterile PBS and fresh DMEM
476 medium supplemented with 400 $\mu\text{g/ml}$ gentamicin was added and retained throughout the
477 infection.

478

479 **Infection of Human Primary Macrophages**

480 Purified monocytes isolated as described from blood of healthy donors were frozen in liquid
481 nitrogen [60,61]. Cells were thawed for experiment and seeded onto 24-well plates at a
482 density of 7×10^5 per well in complete culture medium (RPMI containing 10% FCS) and
483 differentiated into macrophages with rh-M-CSF (10 ng/ml) (purchased from Al-Immuno
484 tools) for 7 days. HMDMs were infected with exponentially growing *P. aeruginosa* cultures
485 ($\text{DO}_{600}=0.8$) at a multiplicity of infection (MOI) of 10:1, as described above.

486

487 **Live microscopy**

488 J774 macrophages were seeded in ibidi μ slide (8 wells) in DMEM medium supplemented
489 with 10% FBS and infected with *P. aeruginosa* PAO1 expressing GFP as described in the
490 previous section. Imaging started after 30 min of phagocytosis, when the media was changed
491 to DMEM supplemented with 400 $\mu\text{g/ml}$ gentamicin until 3 hrs post phagocytosis. Cells were
492 imaged using an inverted epifluorescence microscope (Axioobserver, Zeiss), equipped with
493 an incubation chamber set-up at 37°C and 5% CO_2 and a CoolSNAP HQ2 CCD camera
494 (Photometrics). Time-lapse experiments were performed, by automatic acquisition of random

495 fields using a 63X Apochromat objective (NA 1.4). The frequency of acquisition is indicated
496 in figure legends. Image treatment and analysis were performed using Zen software (Zeiss).

497

498 **Transmission Electron microscopy**

499 Macrophages were seeded on glass coverslips and infected as described above. Infected cells
500 were fixed for 4 hrs at room temperature with 2.5% gluteraldehyde in cacodylate buffer 0.1 M
501 pH 7.4 with 5mM CaCl₂, washed with cacodylate buffer, post-fixed for 1 hr in 1% osmium
502 tetroxide and 1.5 % potassium ferricyanide in cacodylate buffer, washed with distilled water,
503 followed by overnight incubation in 2% uranyl acetate, prepared in water. Dehydration was
504 performed through acetonitrile series and samples were impregnated in epon 118: acetonitrile
505 50:50, followed by two times for 1 hr in 100% epon. After overnight polymerization at 60°C,
506 coverslips were detached by thermal shock with liquid nitrogen. Polymerization was then
507 prolonged for 48 hrs at 60°C. Ultrathin sections of 70 nm were cut with a Leica UC7
508 ultramicrotome (Leica microsystems), counterstained with lead citrate and observed in a Jeol
509 1200 EXII transmission electron microscope. All chemicals were from Electron Microscopy
510 Sciences (USA) and solvents were from Sigma. Images were processed using Fiji software.

511

512 **Colocalization of *P. aeruginosa* with acidic compartments**

513 Macrophages were infected with GFP labelled *P. aeruginosa* as described above. After 2.5
514 hrs of gentamicin treatment, infected J774 cells were washed twice with PBS and incubated
515 with 50 nM LysoTracker red DND-99 (Molecular Probes) in DMEM for 10 min to stain
516 lysosomes. Cells were then washed with PBS and fixed with 4% paraformaldehyde in PBS
517 and mounted on glass slides in Vectashield (Vector Laboratories, Inc) with 4',6-diamidino-2-
518 phenylindole (DAPI) to stain the nucleus. The slides were examined using an upright

519 fluorescence microscope (Axioimager Z2, Zeiss) equipped with an Apotome 1 for optical
520 sectioning. A 63X Apochromat Objective (NA 1.4) was used, transmitted light was acquired
521 using differential interference contrast (DIC), Fluorescein isothiocyanate (FITC) filter was
522 used to visualize GFP expressing bacteria and LysoTracker red fluorescence was acquired
523 using a Texas Red filter set.

524

525 **Phalloidin labeling**

526 J774 macrophages were seeded on glass coverslips and infected with GFP expressing bacteria
527 as described in the previous sections. For cytochalasin treatment, DMEM containing 2 μ M
528 cytochalasin D (Sigma) was added to the macrophages 1 hour before infection and maintained
529 during phagocytosis. After phagocytosis, the cells were maintained in 1 μ M cytochalasin D
530 till the end of the experiment. For untreated control, 0.2 % DMSO (solvent control) in DMEM
531 was added to the cells before and during phagocytosis. After phagocytosis, cells were
532 maintained in 0.1 % DMSO. After fixation with 4% paraformaldehyde (EMS, USA) in PBS
533 for 5 min, cells were washed once with PBS and permeabilized by adding 0.1% Triton X-100
534 for 1 min 30 sec. Cells were then washed once with PBS and incubated with 1 μ g/ml
535 Tetramethylrhodamine B isothiocyanate (TRITC)-labeled phalloidin (Sigma-Aldrich) in PBS
536 for 30 min in dark. Cells were washed twice with PBS and coverslips were mounted on glass
537 slides in Vectashield with DAPI (Vector Laboratories, Inc). The slides were examined using
538 an upright fluorescence microscope (Axioimager Z1, Zeiss) equipped with an Apotome 1 for
539 optical sectioning. A 63X Apochromat Objective (NA 1.4) was used and transmitted light was
540 acquired using DIC. FITC and Texas Red filters were used to visualize GFP expressing bacteria
541 and phalloidin respectively. Cell nuclei were visualized using DAPI filter. Images were
542 processed using ZEN software (Zeiss). Cells were counted manually, where infected cells
543 lacking the phalloidin stain were considered as lysed. Percentage of such lysed cells with

544 intracellular bacteria out of total number of infected cells was calculated and plotted for each
545 strain.

546 Strains containing pSBC6 plasmid (expressing *exsA* under the control of *tac* promoter) were
547 grown before infection in LB or in LB supplemented with 0.01 mM IPTG. Because these
548 strains did not harbor GFP producing plasmid, the number of total cells without phalloidin
549 label was counted and percentage out of total number of cells was plotted. The percent of
550 lysed cells for wild-type strain was similar to that found with GFP positive PAO1 strain.

551

552 **LDH cytotoxicity assay**

553 The cytotoxicity was assessed by release of LDH from infected J774 macrophages infected,
554 using the Pierce LDH cytotoxicity assay kit (Thermo Scientific). Macrophages were infected
555 for 2 hrs at an MOI of 10 as described above, except that cells were seeded in a 96 well plate
556 and extracellular bacteria were not removed. The assay was performed on 50 µl of the culture
557 supernatant according to manufacturer's instructions. LDH release was obtained by
558 subtracting the 680 nm absorbance value from 490 nm absorbance. The percentage of LDH
559 release was first normalized to that of the uninfected control and then calculated relatively to
560 that of uninfected cells lysed with Triton X-100, which was set at 100% LDH release.

561

562 **Trypan Blue exclusion test of cell viability**

563 The membrane impermeable dye Trypan Blue was used to quantify cell viability after
564 phagocytosis or after 2 hrs of gentamicin treatment following phagocytosis. Trypan Blue stain
565 (0.4%) was added in 1:1 ratio with PBS for 3 min at room temperature, replaced by PBS and
566 the cells were imaged using an optical microscope in bright field mode. Dead cells appear
567 blue as they take up the stain, in contrast to healthy cells that appear transparent because of

568 the exclusion of the dye. Cells were counted and the percentage of dead cells out of total cells
569 (blue + colorless) was calculated.

570

571 **RNA extraction and quantitative RT-PCR (qRT-PCR)**

572 For bacterial RNA extraction from infected J774, 6.5×10^6 macrophages were seeded into a
573 100 cm^2 tissue culture dish and infected at an MOI of 10 as described above. 1 hour after
574 phagocytosis, cells were washed three times with PBS, lysed with 0.1% Triton X100 and
575 pelleted by centrifugation at 13000 rpm for 10 min at 15°C . Bacteria were resuspended in 500
576 μl PBS and the non resuspended cellular debris was discarded. 900 μl of RNA protect reagent
577 (Qiagen) was added and incubated for 5 min. The sample was centrifuged at 13000 rpm for
578 10 min. Bacteria in the pellet were lysed with lysozyme and RNA was prepared with RNEasy
579 kit (Qiagen). Superscript III reverse transcriptase (Invitrogen) was used for reverse
580 transcription. Controls without reverse transcriptase were done on each RNA sample to rule
581 out possible DNA contamination. Quantitative real-time PCR (q-RT-PCR) was performed
582 using a Light Cycler 480 SYBR Green I Master mix in a 480 Light Cycler instrument
583 (Roche). PCR conditions were as follows: 3 min denaturation at 98°C , 45 cycles of 98°C for 5
584 sec, 60°C for 10 sec and 72°C for 10 sec. The sequences of primers used for RT-PCR are
585 listed in Table S1.

586

587 **Cyclic di-GMP reporter assay**

588 The strains were transformed by electroporation with the plasmid pCdrA::*gfp* [34,38], which
589 expresses GFP under the control of the promoter of *cdrA*, a c-di-GMP responsive gene, and
590 carries a gentamicin resistance gene. Overnight cultures, grown in LB with $100 \mu\text{g/ml}$
591 gentamicin, were subcultured in LB. These cultures were used to infect J774 cells seeded in a

592 96 well plate (Greiner, Flat-Bottom), containing 10^5 cells per well with an MOI of 20 after
593 normalizing the inoculum to their OD_{600} . After phagocytosis, DMEM containing 300 $\mu\text{g/ml}$
594 of amikacin, instead of gentamicin, was added to eliminate extracellular bacteria, as these
595 strains are resistant to gentamicin. At the required time point, Tecan fluorimeter (Spark 20M)
596 was used to measure fluorescence (excitation, 485 nm and emission, 520 nm) of cells at the Z
597 point where emission peak could be obtained in comparison to the blank. Fluorescence was
598 plotted for each strain in terms of arbitrary units (AU). CdrA activity of all strains was also
599 measured in liquid cultures under changing concentrations of magnesium. All strains, grown
600 overnight in LB, were diluted in LB and grown until OD_{600} of 0.6, washed in NCE medium
601 without magnesium and resuspended in NCE medium containing 1 mM, 10 μM or no
602 magnesium for 1 hour in 96 well plate (Greiner, Flat-Bottom). Their fluorescence (excitation,
603 485 nm and emission, 520 nm) and $OD_{600\text{nm}}$ was measured. Fluorescence ($AU_{520\text{nm}}$) was
604 normalized to $OD_{600\text{nm}}$ and plotted for each strain.

605

606 **CCF4 fluorometric assay to monitor the escape of *P. aeruginosa* in host cytosol**

607 The vacuole escape assay was adapted from the CCF4 FRET assay [43] using the CCF4-AM
608 LiveBlazer Loading Kit (Invitrogen) and an image-based quantification [62]. Briefly, J774
609 macrophages were seeded in 96 well plate (Greiner, Flat-Bottom), containing 5×10^4 cells per
610 well. Overnight bacterial cultures were subcultured in LB with 50 $\mu\text{g/ml}$ of ampicillin to
611 enhance the expression of beta-lactamase, present naturally in *P. aeruginosa*. Infection was
612 carried out as mentioned in the previous sections at the MOI of 10. After phagocytosis, the
613 cells were washed thrice with PBS to remove extracellular bacteria. 100 μl of HBSS buffer
614 containing 3 mM probenecid and gentamicin (400 $\mu\text{g/ml}$), was added in each well. The
615 substrate solution was prepared by mixing 6 μl of CCF4-AM (solution A), 60 μl of solution B
616 and 934 μl of solution C. 20 μl of the substrate solution was added to each well and the plate

617 was incubated in dark at 37 °C with 5% CO₂. After 2 hrs, the cells were imaged as described
618 in the Live Imaging section, using a 10X objective. FITC and DAPI channels were used to
619 visualize CCF4-FRET (Green) and loss of FRET (Blue) respectively. Each sample was taken
620 in triplicate and image acquisition was performed by automated random acquisition. Images
621 were analyzed by Cell Profiler software to calculate the number of blue and green cells. The
622 threshold for detection of blue signal by the software was normalized to uninfected control i.e.
623 no blue cells could be detected in the uninfected control. The percentage of blue cells,
624 representing the cells with cytosolic bacteria, out of total green cells was plotted. All strains
625 were tested for their ability to cleave CCF4 *in vitro*, before carrying out the vacuole rupture
626 assay. Overnight cultures grown in LB were subcultured at the ratio of 1:20 in LB with 100
627 µg/ml of ampicillin. After 2 hours of growth, the cultures were centrifuged and resuspended
628 in PBS. 100 µl of this was aliquoted in 96 well plate (Greiner, Flat-Bottom) and 20 µl of
629 CCF4 substrate solution (A+B+C) was added. Tecan fluorimeter (Spark 20M) was used to
630 measure fluorescence (excitation, 405 nm and emission, 450 nm) using PBS as blank. Blue
631 fluorescence (AU_{450nm}) was observed for all strains and none of the mutants exhibited
632 significantly lower value than the wild-type strain.

633

634 **Ethics statement**

635 Monocytes were issued from blood of anonymous donors obtained from the French blood
636 bank (Etablissement Français du Sang, approval EFS-OCPM n° 21PLER2018-0057).

637

638

639 **Acknowledgments**

640 We thank Sylvie Chevalier (Rouen), Ina Attrée and Sylvie Elsen (Grenoble) for providing
641 strains and plasmids, the Montpellier RIO Imaging microscopy platform for photonic
642 Microscopy and the Electron Microscopy facility of the University of Montpellier (MEA) for
643 sample preparation and transmission electron microscopy. We thank Bérengère Ize and Laila
644 Gannoun-Zaki for critical reading of the manuscript, Matteo Bonazzi and Fernande Siadous
645 for their expertise with the CCF4 assay, Chantal Soscia for testing ExoS secretion.

646

647

648 **References**

649

- 650 1. Silva MT (2012) Classical labeling of bacterial pathogens according to their lifestyle in the host:
651 inconsistencies and alternatives. *Front Microbiol* 3: 71.
- 652 2. Pujol C, Bliska JB (2005) Turning *Yersinia* pathogenesis outside in: subversion of macrophage
653 function by intracellular yersiniae. *Clin Immunol* 114: 216-226.
- 654 3. Kubica M, Guzik K, Koziel J, Zarebski M, Richter W, et al. (2008) A potential new pathway for
655 *Staphylococcus aureus* dissemination: the silent survival of *S. aureus* phagocytosed by human
656 monocyte-derived macrophages. *PLoS One* 3: e1409.
- 657 4. Garzoni C, Kelley WL (2009) *Staphylococcus aureus*: new evidence for intracellular persistence.
658 *Trends Microbiol* 17: 59-65.
- 659 5. Flannagan RS, Heit B, Heinrichs DE (2016) Intracellular replication of *Staphylococcus aureus* in
660 mature phagolysosomes in macrophages precedes host cell death, and bacterial escape and
661 dissemination. *Cell Microbiol* 18: 514-535.
- 662 6. Jubrail J, Morris P, Bewley MA, Stoneham S, Johnston SA, et al. (2016) Inability to sustain
663 intraphagolysosomal killing of *Staphylococcus aureus* predisposes to bacterial persistence in
664 macrophages. *Cell Microbiol* 18: 80-96.
- 665 7. Ercoli G, Fernandes VE, Chung WY, Wanford JJ, Thomson S, et al. (2018) Intracellular replication of
666 *Streptococcus pneumoniae* inside splenic macrophages serves as a reservoir for septicemia.
667 *Nat Microbiol*.
- 668 8. Klockgether J, Tummler B (2017) Recent advances in understanding *Pseudomonas aeruginosa* as a
669 pathogen. *F1000Res* 6: 1261.
- 670 9. Engel J, Balachandran P (2009) Role of *Pseudomonas aeruginosa* type III effectors in disease. *Curr*
671 *Opin Microbiol* 12: 61-66.
- 672 10. Hauser AR (2009) The type III secretion system of *Pseudomonas aeruginosa*: infection by
673 injection. *Nat Rev Microbiol* 7: 654-665.

- 674 11. Feltman H, Schulert G, Khan S, Jain M, Peterson L, et al. (2001) Prevalence of type III secretion
675 genes in clinical and environmental isolates of *Pseudomonas aeruginosa*. *Microbiology* 147:
676 2659-2669.
- 677 12. Garcia-Medina R, Dunne WM, Singh PK, Brody SL (2005) *Pseudomonas aeruginosa* acquires
678 biofilm-like properties within airway epithelial cells. *Infect Immun* 73: 8298-8305.
- 679 13. Sana TG, Hachani A, Bucior I, Soscia C, Garvis S, et al. (2012) The second type VI secretion system
680 of *Pseudomonas aeruginosa* strain PAO1 is regulated by quorum sensing and Fur and
681 modulates internalization in epithelial cells. *J Biol Chem* 287: 27095-27105.
- 682 14. Mittal R, Grati M, Gerring R, Blackwelder P, Yan D, et al. (2014) In vitro interaction of
683 *Pseudomonas aeruginosa* with human middle ear epithelial cells. *PLoS One* 9: e91885.
- 684 15. Kazmierczak BI, Jou TS, Mostov K, Engel JN (2001) Rho GTPase activity modulates *Pseudomonas*
685 *aeruginosa* internalization by epithelial cells. *Cell Microbiol* 3: 85-98.
- 686 16. Angus AA, Lee AA, Augustin DK, Lee EJ, Evans DJ, et al. (2008) *Pseudomonas aeruginosa* induces
687 membrane blebs in epithelial cells, which are utilized as a niche for intracellular replication
688 and motility. *Infect Immun* 76: 1992-2001.
- 689 17. Kroken AR, Chen CK, Evans DJ, Yahr TL, Fleiszig SMJ (2018) The Impact of ExoS on *Pseudomonas*
690 *aeruginosa* Internalization by Epithelial Cells Is Independent of fleQ and Correlates with
691 Bistability of Type Three Secretion System Gene Expression. *MBio* 9.
- 692 18. Angus AA, Evans DJ, Barbieri JT, Fleiszig SM (2010) The ADP-ribosylation domain of *Pseudomonas*
693 *aeruginosa* ExoS is required for membrane bleb niche formation and bacterial survival within
694 epithelial cells. *Infect Immun* 78: 4500-4510.
- 695 19. Heimer SR, Evans DJ, Stern ME, Barbieri JT, Yahr T, et al. (2013) *Pseudomonas aeruginosa* utilizes
696 the type III secreted toxin ExoS to avoid acidified compartments within epithelial cells. *PLoS*
697 *One* 8: e73111.
- 698 20. Lovewell RR, Patankar YR, Berwin B (2014) Mechanisms of phagocytosis and host clearance of
699 *Pseudomonas aeruginosa*. *Am J Physiol Lung Cell Mol Physiol* 306: L591-603.
- 700 21. Brannon MK, Davis JM, Mathias JR, Hall CJ, Emerson JC, et al. (2009) *Pseudomonas aeruginosa*
701 Type III secretion system interacts with phagocytes to modulate systemic infection of
702 zebrafish embryos. *Cell Microbiol* 11: 755-768.
- 703 22. Kumar SS, Tandberg JI, Penesyan A, Elbourne LDH, Suarez-Bosche N, et al. (2018) Dual
704 Transcriptomics of Host-Pathogen Interaction of Cystic Fibrosis Isolate *Pseudomonas*
705 *aeruginosa* PASS1 With Zebrafish. *Front Cell Infect Microbiol* 8: 406.
- 706 23. Schmiedl A, Kerber-Momot T, Munder A, Pabst R, Tschernig T (2010) Bacterial distribution in lung
707 parenchyma early after pulmonary infection with *Pseudomonas aeruginosa*. *Cell Tissue Res*
708 342: 67-73.
- 709 24. Buyck JM, Tulkens PM, Van Bambeke F (2013) Pharmacodynamic evaluation of the intracellular
710 activity of antibiotics towards *Pseudomonas aeruginosa* PAO1 in a model of THP-1 human
711 monocytes. *Antimicrob Agents Chemother* 57: 2310-2318.
- 712 25. Belon C, Soscia C, Bernut A, Laubier A, Bleves S, et al. (2015) A Macrophage Subversion Factor Is
713 Shared by Intracellular and Extracellular Pathogens. *PLoS Pathog* 11: e1004969.
- 714 26. Mittal R, Lisi CV, Kumari H, Grati M, Blackwelder P, et al. (2016) Otopathogenic *Pseudomonas*
715 *aeruginosa* Enters and Survives Inside Macrophages. *Front Microbiol* 7: 1828.
- 716 27. Bernut A, Belon C, Soscia C, Bleves S, Blanc-Potard AB (2015) Intracellular phase for an
717 extracellular bacterial pathogen: MgtC shows the way. *Microb Cell* 2: 353-355.
- 718 28. Lee EJ, Pontes MH, Groisman EA (2013) A bacterial virulence protein promotes pathogenicity by
719 inhibiting the bacterium's own F1Fo ATP synthase. *Cell* 154: 146-156.
- 720 29. Pontes MH, Lee EJ, Choi J, Groisman EA (2015) *Salmonella* promotes virulence by repressing
721 cellulose production. *Proc Natl Acad Sci U S A* 112: 5183-5188.
- 722 30. Alix E, Blanc-Potard AB (2007) MgtC: a key player in intramacrophage survival. *Trends Microbiol*
723 15: 252-256.
- 724 31. Belon C, Blanc-Potard AB (2016) Intramacrophage Survival for Extracellular Bacterial Pathogens:
725 MgtC As a Key Adaptive Factor. *Front Cell Infect Microbiol* 6: 52.

- 726 32. Fito-Boncompte L, Chapalain A, Bouffartigues E, Chaker H, Lesouhaitier O, et al. (2011) Full
727 virulence of *Pseudomonas aeruginosa* requires OprF. *Infect Immun* 79: 1176-1186.
- 728 33. Chevalier S, Bouffartigues E, Bodilis J, Maillot O, Lesouhaitier O, et al. (2017) Structure, function
729 and regulation of *Pseudomonas aeruginosa* porins. *FEMS Microbiol Rev* 41: 698-722.
- 730 34. Bouffartigues E, Moscoso JA, Duchesne R, Rosay T, Fito-Boncompte L, et al. (2015) The absence of
731 the *Pseudomonas aeruginosa* OprF protein leads to increased biofilm formation through
732 variation in c-di-GMP level. *Front Microbiol* 6: 630.
- 733 35. Ince D, Sutterwala FS, Yahr TL (2015) Secretion of Flagellar Proteins by the *Pseudomonas*
734 *aeruginosa* Type III Secretion-Injectisome System. *J Bacteriol* 197: 2003-2011.
- 735 36. Soscia C, Hachani A, Bernadac A, Filloux A, Bleves S (2007) Cross talk between type III secretion
736 and flagellar assembly systems in *Pseudomonas aeruginosa*. *J Bacteriol* 189: 3124-3132.
- 737 37. Moscoso JA, Mikkelsen H, Heeb S, Williams P, Filloux A (2011) The *Pseudomonas aeruginosa*
738 sensor RetS switches type III and type VI secretion via c-di-GMP signalling. *Environ Microbiol*
739 13: 3128-3138.
- 740 38. Rybtke MT, Borlee BR, Murakami K, Irie Y, Hentzer M, et al. (2012) Fluorescence-based reporter
741 for gauging cyclic di-GMP levels in *Pseudomonas aeruginosa*. *Appl Environ Microbiol* 78:
742 5060-5069.
- 743 39. Coburn J, Frank DW (1999) Macrophages and epithelial cells respond differently to the
744 *Pseudomonas aeruginosa* type III secretion system. *Infect Immun* 67: 3151-3154.
- 745 40. Franchi L, Stoolman J, Kanneganti TD, Verma A, Ramphal R, et al. (2007) Critical role for Ipaf in
746 *Pseudomonas aeruginosa*-induced caspase-1 activation. *Eur J Immunol* 37: 3030-3039.
- 747 41. Galle M, Schotte P, Haegman M, Wullaert A, Yang HJ, et al. (2008) The *Pseudomonas aeruginosa*
748 Type III secretion system plays a dual role in the regulation of caspase-1 mediated IL-1 β
749 maturation. *J Cell Mol Med* 12: 1767-1776.
- 750 42. Huber P, Bouillot S, Elsen S, Attree I (2014) Sequential inactivation of Rho GTPases and Lim kinase
751 by *Pseudomonas aeruginosa* toxins ExoS and ExoT leads to endothelial monolayer
752 breakdown. *Cell Mol Life Sci* 71: 1927-1941.
- 753 43. Keller C, Mellouk N, Danckaert A, Simeone R, Brosch R, et al. (2013) Single cell measurements of
754 vacuolar rupture caused by intracellular pathogens. *J Vis Exp*: e50116.
- 755 44. Tsutsumi Y, Tomita H, Tanimoto K (2013) Identification of novel genes responsible for
756 overexpression of ampC in *Pseudomonas aeruginosa* PAO1. *Antimicrob Agents Chemother*
757 57: 5987-5993.
- 758 45. Hritonenko V, Evans DJ, Fleiszig SM (2012) Translocon-independent intracellular replication by
759 *Pseudomonas aeruginosa* requires the ADP-ribosylation domain of ExoS. *Microbes Infect* 14:
760 1366-1373.
- 761 46. Landeta C, Boyd D, Beckwith J (2018) Disulfide bond formation in prokaryotes. *Nat Microbiol* 3:
762 270-280.
- 763 47. Vareechon C, Zmina SE, Karmakar M, Pearlman E, Rietsch A (2017) *Pseudomonas aeruginosa*
764 Effector ExoS Inhibits ROS Production in Human Neutrophils. *Cell Host Microbe* 21: 611-618
765 e615.
- 766 48. Hauser AR, Engel JN (1999) *Pseudomonas aeruginosa* induces type-III-secretion-mediated
767 apoptosis of macrophages and epithelial cells. *Infect Immun* 67: 5530-5537.
- 768 49. Dacheux D, Toussaint B, Richard M, Brochier G, Croize J, et al. (2000) *Pseudomonas aeruginosa*
769 cystic fibrosis isolates induce rapid, type III secretion-dependent, but ExoU-independent,
770 oncosis of macrophages and polymorphonuclear neutrophils. *Infect Immun* 68: 2916-2924.
- 771 50. Vance RE, Rietsch A, Mekalanos JJ (2005) Role of the type III secreted exoenzymes S, T, and Y in
772 systemic spread of *Pseudomonas aeruginosa* PAO1 in vivo. *Infect Immun* 73: 1706-1713.
- 773 51. Sutterwala FS, Mijares LA, Li L, Ogura Y, Kazmierczak BI, et al. (2007) Immune recognition of
774 *Pseudomonas aeruginosa* mediated by the IPAF/NLRC4 inflammasome. *J Exp Med* 204: 3235-
775 3245.

- 776 52. Balakrishnan A, Karki R, Berwin B, Yamamoto M, Kanneganti TD (2018) Guanylate binding
777 proteins facilitate caspase-11-dependent pyroptosis in response to type 3 secretion system-
778 negative *Pseudomonas aeruginosa*. *Cell Death Discov* 5: 3.
- 779 53. Kaminski A, Gupta KH, Goldufsky JW, Lee HW, Gupta V, et al. (2018) *Pseudomonas aeruginosa*
780 ExoS Induces Intrinsic Apoptosis in Target Host Cells in a Manner That is Dependent on its
781 GAP Domain Activity. *Sci Rep* 8: 14047.
- 782 54. Pederson KJ, Vallis AJ, Aktories K, Frank DW, Barbieri JT (1999) The amino-terminal domain of
783 *Pseudomonas aeruginosa* ExoS disrupts actin filaments via small-molecular-weight GTP-
784 binding proteins. *Mol Microbiol* 32: 393-401.
- 785 55. Wood SJ, Goldufsky JW, Bello D, Masood S, Shafikhani SH (2015) *Pseudomonas aeruginosa* ExoT
786 Induces Mitochondrial Apoptosis in Target Host Cells in a Manner That Depends on Its
787 GTPase-activating Protein (GAP) Domain Activity. *J Biol Chem* 290: 29063-29073.
- 788 56. Sawa T, Shimizu M, Moriyama K, Wiener-Kronish JP (2014) Association between *Pseudomonas*
789 *aeruginosa* type III secretion, antibiotic resistance, and clinical outcome: a review. *Crit Care*
790 18: 668.
- 791 57. Munzenmayer L, Geiger T, Daiber E, Schulte B, Autenrieth SE, et al. (2016) Influence of Sae-
792 regulated and Agr-regulated factors on the escape of *Staphylococcus aureus* from human
793 macrophages. *Cell Microbiol* 18: 1172-1183.
- 794 58. Rang C, Alix E, Felix C, Heitz A, Tasse L, et al. (2007) Dual role of the MgtC virulence factor in host
795 and non-host environments. *Mol Microbiol* 63: 605-622.
- 796 59. Nivens DE, Ohman DE, Williams J, Franklin MJ (2001) Role of alginate and its O acetylation in
797 formation of *Pseudomonas aeruginosa* microcolonies and biofilms. *J Bacteriol* 183: 1047-
798 1057.
- 799 60. Bessoles S, Dudal S, Besra GS, Sanchez F, Lafont V (2009) Human CD4+ invariant NKT cells are
800 involved in antibacterial immunity against *Brucella suis* through CD1d-dependent but CD4-
801 independent mechanisms. *Eur J Immunol* 39: 1025-1035.
- 802 61. Gannoun-Zaki L, Alibaud L, Carrere-Kremer S, Kremer L, Blanc-Potard AB (2013) Overexpression
803 of the KdpF membrane peptide in *Mycobacterium bovis* BCG results in reduced
804 intramacrophage growth and altered cording morphology. *PLoS One* 8: e60379.
- 805 62. Martinez E, Allombert J, Cantet F, Lakhani A, Yandrapalli N, et al. (2016) *Coxiella burnetii* effector
806 CvpB modulates phosphoinositide metabolism for optimal vacuole development. *Proc Natl*
807 *Acad Sci U S A* 113: E3260-3269.

808

809

810

811 **Figure legends**

812

813 **Fig 1. Live imaging of macrophages infected with *P. aeruginosa*.** J774 macrophages were
814 infected with PAO1 wild-type (WT) strain expressing GFP. Time lapse imaging was started at
815 1.5 hrs post-phagocytosis. Cells were maintained in DMEM supplemented with gentamicin at
816 37°C and 5% CO₂ throughout imaging. White arrows point at the cells that harbor
817 intracellular bacteria and undergo lysis between 1.5 hrs and 3 hrs post-phagocytosis. Black
818 arrow shows an uninfected and unlyed cell. Scale bar is equivalent to 10 μm.

819

820 **Fig 2. Transmission electron micrographs (TEM) of *P. aeruginosa* within macrophages.**
821 J774 macrophages were infected with *P. aeruginosa* for 30 min (A) or 3 hrs (B and C) and
822 subjected to TEM (left panels). Black rectangles show intracellular bacteria that are shown at
823 higher magnification in the right panels. A. At early time after phagocytosis, most of bacteria
824 were found inside membrane bound vacuoles (white arrows). B. At later time, some bacteria
825 can be observed in the cytoplasm with no surrounding membrane suggesting disruption of the
826 vacuole membrane (black arrows). The infected macrophage in panel B shows an abnormal
827 morphology, with highly condensed chromatin and membrane blebbing, but no pseudopodia.
828 C. At later time, bacteria can also be found in vacuole partially or totally filled with
829 heterogeneous electron dense material (white arrows), suggesting that the vacuole has fused
830 with lysosomes. The infected macrophage shown in panel C appears normal.

831

832 **Fig 3. Visualization (A) and quantification (B) of lysed infected cells upon phalloidin**
833 **labeling.** GFP expressing PAO1 WT, Δ *mgtC* and Δ *oprF* strains were used for infecting J774
834 macrophages. Gentamicin was added after phagocytosis and cells were fixed at 2 hrs post-
835 phagocytosis, stained with phalloidin and imaged with fluorescent microscope. DAPI was

836 used to stain the nucleus. Cells that have intracellular bacteria, but lack the phalloidin cortical
837 label were considered as lysed by intracellular bacteria (shown by arrows). Scale bar is
838 equivalent to 10 μm . After imaging, infected cells were counted and percentage of lysed cells
839 with intracellular bacteria out of total number of cells was plotted for each strain. Error bars
840 correspond to standard errors from three independent experiments. At least 200 cells were
841 counted per strain. The asterisks indicate P values (One way ANOVA, where all strains were
842 compared to WT using Dunnet's multiple comparison post-test, $*P < 0.05$ and $***P < 0.001$),
843 showing statistical significance with respect to WT.

844

845 **Fig 4. Expression of T3SS genes in *P. aeruginosa* strains residing in J774 macrophages.**
846 J774 macrophages were infected with PAO1 WT, ΔmgtC and ΔoprF strains. After
847 phagocytosis, cells were maintained in DMEM supplemented with gentamicin. RNA was
848 extracted from bacteria isolated from infected macrophages 1 hr after phagocytosis. The level
849 of *exoS*, *pcrV* and *fliC* transcripts relative to those of the house-keeping gene *rpoD* was
850 measured by qRT-PCR and plotted on the Y-axis. Error bars correspond to standard errors
851 from at least three independent experiments. The asterisks indicate P values (One way
852 ANOVA, where all strains were compared to WT using Dunnet's multiple comparison post-
853 test, $*P < 0.05$, $**P < 0.01$, $***P < 0.001$ and ns = $P > 0.05$ or non-significant), showing
854 statistical significance with respect to WT.

855

856 **Fig 5. Measurement of c-di-GMP level in ΔmgtC and ΔoprF mutants.** PAO1 WT, ΔmgtC
857 and ΔoprF harboring reporter plasmid pCdrA::*gfp*, which expresses GFP under the control of
858 the promoter of c-di-GMP responsive gene *cdrA* (A), were used to infect J774 cells and
859 fluorescence was measured (B). After phagocytosis, DMEM containing 300 $\mu\text{g/ml}$ of

860 amikacin was added to eliminate extracellular bacteria. Fluorescence (excitation, 485 nm and
861 emission, 520 nm) was measured 1 hour after phagocytosis and plotted as arbitrary units
862 (AU). Error bars correspond to standard errors from four independent experiments. The
863 asterisks indicate *P* values (One way ANOVA, where all strains were compared to WT using
864 Dunnet's multiple comparison post-test, **P* <0.05 and ****P* <0.001), showing statistical
865 significance with respect to WT. C. PAO1 WT, Δ *mgtC* and Δ *oprF* harboring reporter plasmid
866 pCdrA::*gfp*, were grown in NCE medium with varying concentration of Mg²⁺. After 1 hour of
867 growth, fluorescence (excitation, 485 nm and emission, 520 nm) of the culture was measured
868 along with its O.D_{600nm}. The fluorescence was plotted as arbitrary units (AU_{520nm}) after
869 normalizing with O.D_{600nm} (C). Error bars correspond to standard errors from three
870 independent experiments. The asterisks indicate *P* values showing statistical significance with
871 respect to WT in the respective condition, using Student's t test (ns = *P* >0.05, **P* <0.05, ***P*
872 <0.01 and ****P* <0.001).

873

874 **Fig 6. Assessment of role of T3SS and its effectors in cell lysis induced by intracellular**
875 **PAO1.** J774 macrophages were infected with GFP expressing strains as indicated. After
876 phagocytosis, cells were maintained in DMEM supplemented with gentamicin. Cells were
877 imaged 2 hrs post-phagocytosis after staining with phalloidin (A). Scale bar is equivalent to
878 10 μ m. Lysis was quantified (B & C) by counting infected cells lacking cortical labeling
879 (indicated by arrows). Percentage of lysed cells with intracellular bacteria out of total number
880 of cells was plotted. Error bars correspond to standard errors from at least three independent
881 experiments. At least 200 cells were counted per strain. The asterisks indicate *P* values (One
882 way ANOVA, where all strains were compared to WT using Dunnet's multiple comparison
883 test, ****P* <0.001), showing statistical significance with respect to WT.

884

885 **Fig 7. Visualization and quantification of lysis of infected primary human macrophages**
886 **driven intracellularly by *P. aeruginosa* strains.** HMDMs were infected with GFP
887 expressing PAO1 WT, $\Delta oprF$, and \DeltapscN strains. After phagocytosis, cells were maintained
888 in RPMI supplemented with gentamicin. Cells were imaged 2 hrs post-phagocytosis after
889 staining with phalloidin (A) and lysis was quantified (B) by counting infected cells lacking
890 cortical labeling (indicated by arrows). Scale bar is equivalent to 10 μ m. Percentage of lysed
891 cells with intracellular bacteria out of total number of cells was plotted. Error bars correspond
892 to standard errors from two independent experiments. At least 200 cells were counted per
893 strain. The asterisks indicate *P* values (One way ANOVA, where all strains were compared to
894 WT using Bonferroni's multiple comparison test, $***P < 0.001$), showing statistical
895 significance with respect to WT.

896

897 **Fig 8. Assessment of access of *P. aeruginosa* to host cytosol using phagosome escape**
898 **assay.** J774 macrophages were infected with PAO1 WT, $\Delta mgtC$, $\Delta oprF$ and \DeltapscN strains.
899 After phagocytosis, cells were stained with CCF4-AM in presence of gentamicin. 2 hours
900 post-phagocytosis, the cells were imaged with 10X objective using FITC and DAPI channels.
901 Upon escape of bacteria from phagosome to the cytosol, the CCF4-AM FRET is lost,
902 producing blue color. **A.** Representative pictures are shown with the following channels: Total
903 cell population is shown in merged green and blue cells, whereas cells with cleaved CCF4
904 probe are shown in blue in the lower panel. Scale bar is equivalent to 50 μ m. **B.** Images were
905 analyzed and quantified by Cell Profiler software to calculate the percentage of blue cells out
906 of total green cells. At least 200 cells were counted per strain. Error bars correspond to
907 standard errors from three independent experiments. The asterisks indicate *P* values (One way
908 ANOVA, where all strains were compared to WT using Dunnet's multiple comparison post-
909 test, $**P < 0.01$ and $***P < 0.001$), showing statistical significance with respect to WT. **C.**

910 Electron micrograph showing a disrupted vacuole membrane (white arrows) in a macrophage
911 infected with PAO1 strain. The right panel shows higher magnification of the black square in
912 the left panel.

913

914 **Fig 9. Model for intramacrophage fate of *P. aeruginosa*.** Phagocytosed *P. aeruginosa*
915 PAO1 first resides in a vacuole, before escaping the phagosome and promoting macrophage
916 lysis. This cell lysis driven by intracellular *P. aeruginosa* involves the T3SS and more
917 specifically ExoS. MgtC and OprF act positively on the expression of T3SS, possibly by
918 reducing c-di-GMP level, a negative regulator of T3SS expression. Thereby T3SS and its
919 effector ExoS play a role in phagosomal escape and cell lysis. Further work will be required
920 to address secretion of ExoS from intracellularly expressed T3SS as well as identify host-
921 targets.

922

923

924 **Supporting Information**

925 **S1 Fig. Live imaging of macrophages infected with *P. aeruginosa*.** J774 macrophages were
926 infected with PAO1 wild-type strain expressing GFP. Time lapse imaging was started at 1.5
927 hrs post-phagocytosis. Cells were maintained in DMEM supplemented with gentamicin, at 37
928 °C and 5% CO₂ throughout imaging. White arrows point at infected cells that undergo lysis,
929 whereas black arrows indicate uninfected cells that do not lyse. Images were taken between
930 1.5 hrs and 3 hrs post-phagocytosis as shown on the panels. Scale bar is equivalent to 10 μm.

931

932 **S2 Fig. Live imaging of primary human macrophages infected with *P. aeruginosa*.**
933 HMDMs were infected with PAO1 wild-type (WT) strain expressing GFP. Time lapse
934 imaging was started at 1.5 hrs post-phagocytosis. Cells were maintained in RPMI
935 supplemented with gentamicin at 37°C and 5% CO₂ throughout imaging. White arrows point
936 at the cells that harbor intracellular bacteria and undergo lysis between 1.5 hrs and 3 hrs post-
937 phagocytosis. Black arrow shows an uninfected and unlysed cell. Scale bar is equivalent to 20
938 μm.

939

940 **S3 Fig. Colocalization of *P. aeruginosa* with a probe that labels acidic compartments.**
941 J774 macrophages were infected with PAO1 expressing GFP. After 2.5 hrs of gentamicin
942 treatment, infected J774 cells were incubated with LysoTracker for 10 min, a red fluorescent
943 weak base that accumulates in acidic compartments. Cells were then fixed and imaged with
944 fluorescence microscope. (A) The image shows individual panels for Differential Interference
945 Contrast (DIC), lysosomal compartment (red), bacteria expressing GFP (green), the nucleus
946 (blue) and merged image of all channels. The solid arrow shows colocalization of bacteria

947 with lysotracker and dashed arrow shows non-colocalization. Scale bar is equivalent to 5 μm .
948 (B) 3D-reconstructed image of the same area of (A).

949

950 **S4 Fig. Visualization (A) and quantification (B) of lysed infected cells upon cytochalasin**
951 **D treatment.** GFP expressing PAO1 used for infecting J774 macrophages. DMEM
952 containing 2 μM cytochalasin D was added to the macrophages 1 hour before infection and
953 maintained during phagocytosis. After phagocytosis, cells were maintained in 1 μM
954 cytochalasin D in DMEM supplemented with gentamicin till the end of the experiment. 0.2 %
955 DMSO in DMEM was added to the cells as solvent control before and during phagocytosis.
956 After phagocytosis, cells were maintained in 0.1 % DMSO in DMEM with gentamicin, fixed
957 2 hrs post-phagocytosis, stained with phalloidin and imaged with fluorescent microscope.
958 DAPI was used to stain the nucleus. Cells that have intracellular bacteria, but lack the
959 phalloidin cortical label, were considered as lysed by intracellular bacteria (shown by arrows).
960 Scale bar is equivalent to 10 μm . Percentage of lysed cells with intracellular bacteria out of
961 total number of cells was plotted. Error bars correspond to standard errors from two
962 independent experiments. At least 200 cells were counted per strain. The asterisks indicate *P*
963 values (Student's t-test, *****P* < 0.01**), showing statistical significance with respect to DMSO
964 control.

965

966 **S5 Fig. Quantification of dying cells infected with *P. aeruginosa* strains overexpressing**
967 ***exsA*.** PAO1 WT, ΔoprF , PAO1 WT + *pexsA* and ΔoprF + *pexsA* strains were used for
968 infecting J774 macrophages. Expression of *exsA* was induced by adding 0.01 mM IPTG for
969 the strains PAO1 WT + *pexsA* and ΔoprF + *pexsA*. Gentamicin was added after phagocytosis
970 and cells were fixed at 2 hrs post-phagocytosis, stained with phalloidin and imaged with

971 fluorescent microscope. DAPI was used to stain the nucleus. Cells that lack the phalloidin
972 cortical label were considered as lysed by intracellular bacteria. After imaging, percentage of
973 lysed cells out of total number of cells was plotted for each strain. Error bars correspond to
974 standard errors from at least three independent experiments. At least 200 cells were counted
975 per strain. The asterisks indicate P values (One way ANOVA, where all strains were
976 compared to each other using Bonferroni's multiple comparison post-test, $**P < 0.01$ and $ns =$
977 $P > 0.05$), showing statistical significance with respect to WT.

978

979 **S6 Fig. Quantification of cell lysis driven by extracellular bacteria.** Release of LDH was
980 measured from J774 macrophages infected for 2 hrs with PAO1 WT, $\Delta pscN$, $\Delta exoS$ and
981 $\Delta exoSTY$ mutant strains to quantify the cytotoxicity. The percentage of LDH release was
982 calculated relatively to that of total uninfected cells lysed with Triton X-100, which was set at
983 100% LDH release. Error bars correspond to standard errors (SE) from at least four
984 independent experiments. The asterisks indicate P values (One way ANOVA, where all
985 strains were compared to WT using Dunnet's multiple comparison post-test, $**P < 0.01$),
986 showing statistical significance with respect to WT.

987

988 **S7 Fig. Quantification of lysed cells by staining with Trypan Blue.** J774 macrophages
989 were infected with the strains as indicated. After phagocytosis, cells were maintained in
990 DMEM supplemented with gentamicin. Cells were stained with trypan blue at (A) 30 min or
991 (B) 2 hrs post-phagocytosis and imaged. Lysed cells were quantified by counting cells stained
992 with trypan blue and the percentage of lysed cells out of total number of cells was plotted.
993 Error bars correspond to standard errors from at least three independent experiments. At least
994 400 cells were counted per strain. The asterisks indicate P values (One way ANOVA, where

995 all strains were compared to WT using Dunnet's multiple comparison test, * $P < 0.05$, ** P
996 < 0.01 and *** $P < 0.001$), showing statistical significance with respect to WT.

997

998 **S8 Fig. Assessment of β -lactamase activity in liquid culture.** PAO1 WT, Δ *mgcC*, Δ *oprF*,
999 Δ *pscN*, Δ *exoS* and Δ *exoSTY* strains grown in presence of ampicillin, were incubated with
1000 CCF4-AM for 1 hour. The blue fluorescence generated as a result of loss of FRET of CCF4
1001 was measured (excitation, 420 nm and emission, 450 nm) and plotted as arbitrary units (AU).
1002 Error bars correspond to standard errors from four independent experiments. All strains were
1003 compared to WT using One way ANOVA, Dunnet's multiple comparison post-test. No
1004 significant difference was found between the mutant strains and WT.

1005

1006 **S9 Fig. Phagosome escape assay of T3SS mutants.** J774 macrophages were infected with
1007 PAO1 WT, Δ *pscN*, Δ *exoS* and Δ *exoSTY* strains. After phagocytosis, cells were stained with
1008 CCF4-AM in presence of gentamicin. 2 hours post-phagocytosis, the cells were imaged with
1009 10X objective using FITC and DAPI channels. Upon escape of bacteria from phagosome to
1010 the cytosol, the CCF4-AM FRET is lost, producing blue color. Images were analyzed and
1011 quantified by Cell Profiler software to calculate the percentage of blue cells out of total green
1012 cells. At least 200 cells were counted per strain. Error bars correspond to standard errors from
1013 four independent experiments. The asterisks indicate P values (One way ANOVA, where all
1014 strains were compared to WT using Dunnet's multiple comparison post-test , * $P < 0.05$),
1015 showing statistical significance with respect to WT.

1016

1017 **S10 Fig. Comparison of secreted protein profiles and ExoS production under T3SS-**
1018 **inducing conditions in two PAO1 strains.** Immunodetection of the ExoS effector in culture

1019 supernatant of PAO1 (S. Bleves) and PAO1 H103 (isogenic WT strain for *oprF* mutant)
1020 grown in exponential phase at 37°C under T3SS-inducing ($- Ca^{2+}$) or non-inducing ($+ Ca^{2+}$)
1021 conditions. The bacterial culture equivalent of 0.1 or 1 OD₆₀₀ unit was loaded on an SDS gel
1022 containing 10% polyacrylamide. As control, cellular fraction (equivalent of 0.1 OD₆₀₀ unit
1023 was loaded). Upper panels show Western blot using anti-ExoS antibodies (Soscia et al., 2007;
1024 doi: [10.1128/JB.01677-06](https://doi.org/10.1128/JB.01677-06)) and lower panels show Coomassie stained gels.

1025

1026

1027 **S1 Movie. Live microscopy movie imaging cell lysis in real time.** J774 macrophages were
1028 infected with PAO1 WT strain expressing GFP. Cells were maintained in DMEM
1029 supplemented with gentamicin, at 37 °C and 5% CO₂ throughout imaging. Imaging was
1030 started at 3 hrs post-phagocytosis and continued for 10 min with interval of 30 sec between
1031 frames. The time frame is displayed in the movie in the format of minutes:seconds.milli
1032 seconds. The movie shows quick lysis of macrophages harboring intracellular bacteria
1033 occurring within a minute.

1034

1035 **S1 Table. List of primers used for RT-PCR.**

1036